# Progress on yttria-stabilized zirconia sensors for hydrothermal pH measurements

S.N. Lvov[a,b,*], X.Y. Zhou[b], G.C. Ulmer[c], H.L. Barnes[b,d], D.D. Macdonald[e], S.M. Ulyanov[b], L.G. Benning[d,1], D.E. Grandstaff[c], M. Manna[c], E. Vicenzi[f,2]

[a]Department of Energy and Geo-Environmental Engineering, Pennsylvania State University, University Park, PA 16802, USA
[b]The Energy Institute, Pennsylvania State University, University Park, PA 16802, USA
[c]Department of Geology, Temple University, Philadelphia, PA 19122, USA
[d]Department of Geosciences, Pennsylvania State University, University Park, PA 16802, USA
[e]Department of Materials Science and Engineering, Pennsylvania State University, University Park, PA 16802, USA
[f]Princeton Materials Institute, Princeton University, Princeton, NJ 08540, USA

## Abstract

Electrochemical cells are reviewed and a new design is evaluated for potentiometric pH measurements to above 300 °C. The new design system minimizes the effects of metal corrosion on measured pH. In addition, a recently developed [Zhou, X.Y., Lvov, S.N., Ulyanov, S.M., 2003. Yttria-Stabilized Zirconia Membrane Electrode, US Patent #6, S17, 694] flow-through, yttria-stabilized zirconia (YSZ) pH sensor has been further tested. The Nernstian behavior and precision of the YSZ electrode were evaluated by measuring the potentials vs. $H_2$–Pt electrode at 320 and 350 °C. Also, using the YSZ electrode, the association constants of HCl(aq) at 320 and 350 °C have been determined from the potentials of a HCl(aq) solutions at 0.01 to 0.001 mol kg$^{-1}$. The results, $pK_{320} = -1.46 \pm 0.46$ and $pK_{350} = -2.35 \pm 0.25$, in good agreement with literature data, both demonstrate the effective use of the cell and YSZ electrode for pH measurements to about $\pm 0.05$ pH units, and confirm the Nernstian behavior of the YSZ electrode in acidic HCl solutions up to 350 °C. Commercial YSZ tubes available for high-temperature pH sensing are, however, far from ideal because of irregular compositions, phase structures, and interstitial materials. A consequence is the premature structural decay of YSZ tubes in acidic solutions at elevated temperatures. In spite of the long-term decay, YSZ sensors respond rapidly to changes in pH, apparently limited only by the rate of mixing of solutions within the cell. This system makes the measurement feasible above 300 °C of mineral hydrolysis equilibrium constants and their free energy changes within uncertainties of about $\pm 1.0$ kJ.
© 2003 Elsevier Science B.V. All rights reserved.

Keywords: High temperature; Electrochemical cells; Hydrothermal solutions; Yttria-stabilized zirconia pH sensor; Association constants of HCl(aq)

* Corresponding author. Department of Energy and Geo-Environmental Engineering, The Energy Institute, Pennsylvania State University, 207 Hosler Building, University Park, PA 16802, USA. Fax: +1-814-865-3248.
E-mail address: lvov@psu.edu (S.N. Lvov).
[1] Present address: School of Earth Sciences, University of Leeds, Leeds, LS2 9JT, UK.
[2] Present address: National Museum of Natural History, Smithsonian Institution, Washington, DC 20560, USA.

## 1. Introduction

Direct, precise potentiometric pH measurements at temperatures above 300 °C are difficult to achieve, and hence are not made on a routine basis. If such measurements could be made easily, the data obtained would remarkably improve our understanding of the chemistry of hydrothermal systems. Techniques for high $P$, $T$ (>300 °C) measurements of pH with a precision of $\pm$ 0.05 pH units make possible high quality measured equilibrium constants for acid–base dissociation possible, ion-pairing, hydrolysis, and solubility reactions and the associated standard thermodynamic properties. Precise pH measurements can also be used to evaluate the rates, stoichiometries, and thermodynamics of reactions controlling aqueous speciation, dissolution, precipitation, and mineral alteration in both high-temperature subcritical and supercritical aqueous solutions. Such data help quantify hydrothermal processes in oceanic fluid vents, many ore-forming processes, petrologic metasomatism, deep brines of sedimentary basins, geothermal power plants, supercritical water oxidation systems for the destruction of organic waste, power plant corrosion, and in many other environments.

Of the equilibrium constants needed to quantify solute speciation in hydrothermal fluids, relatively few have been measured at temperatures above 300 °C and then often with unsatisfactory accuracy (Schoonen and Barnes, 1997). With precise pH measurements, equilibrium constants of several types of reactions could be evaluated with significantly improved accuracy. For example, the equilibrium constant of the geochemically common hydrolysis reaction among feldspar, mica and quartz,

$$3/2KAlSi_3O_8(s) + H^+ \rightarrow 1/2KA1_3Si_3O_{10}(OH)_2(s)$$
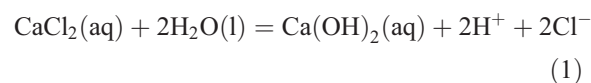$$+ 3SiO_2(s) + K^+$$
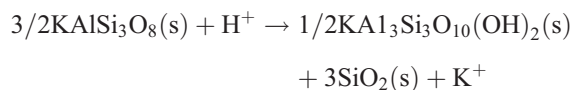
can be determined experimentally by hydrothermal equilibration among (1) the three solids with structural and surface-area energy-minimized, and (2) a selected aqueous concentration of KCl plus (3) a measured pH. Assuming reasonably, a negligible uncertainty for the calculated $K^+$ activity and a measured pH uncertainty

of $\pm$ 0.05, log $K$ in hydrothermal solutions should also be resolved to $\pm$ 0.05, or to less than $\pm$ 1 kJ at 350 °C, a major improvement over such data presently available. As examples of the uncertainties in some related reactions and their evaluation, see Haselton et al. (1995).

Such equilibria are known above about 100 °C from approximate extrapolations. Precise data for *ion-pairing constants*, of which few are currently available, would be obtainable. These data are required, because they strongly affect both ionic strength and ligand activities. Similar needs exist for *complexation constants* (compiled in Seward and Barnes, 1997), which are often unmeasured or imprecisely determined by even our best current methods.

The method by which constants for ion-pairing equilibria can be determined from pH measurements is not necessarily obvious. An example is given by the species $Ca^{2+}$–$CaCl^+$–$CaCl_2$ in the reactions:

$$CaCl_2(aq) + 2H_2O(l) = Ca(OH)_2(aq) + 2H^+ + 2Cl^-$$
$$(1)$$

and

$$CaCl^+ + 2H_2O(l) = Ca(OH)_2(aq) + 2H^+ + Cl^- \quad (2)$$

whose $K$ values can be derived from pH data after verifying, again by pH measurements, the constants for the dissociation of $Ca(OH)_2(aq)$ and $Ca(OH)^+$. These equilibria generally determine whether calcite solubility is prograde or retrograde and, therefore, are especially important geochemically.

Electrodes that are to be used above 300 °C require several major improvements if they are to be of general utility. These include better precision, easier calibration, and improved durability and robustness. Especially for YSZ electrode, information is needed on solutes, which interfere with pH measurements and on temperature and redox limitations of the pH response (Bourcier et al., 1987). To achieve these goals, the principle adopted here is to use a flow-through technique that has already proven to be effective in high-temperature calorimeters, densitometers (Wood et al., 1991), conductance meters (Zimmerman et al., 1995), and electrochemical concentration cells (Sweeton et al., 1973). This

principle minimizes interference from both contamination and the Soret effect (associated with the reference electrode), and should make possible long-term measurements if the ceramic electrode tubes have negligible corrosion rates. Our design has evolved from a configuration that has proven to be effective in developing a high precision reference electrode, as described by Lvov and Zhou (1998) and Lvov et al. (1998a,b, 1999). The adaptation of the flow-through system is described in detail here including both its calibration and some results from its use with halide solutions.

An effective primary sensor is the YSZ electrode using an 8 mol% $Y_2O_3$-stabilized zirconia tube. However, our analyses of commercial tubes for these electrodes revealed that they are subject to degradation from possible leaching of yttria, glass, and other interstitial phases (see Section 3). The texture and composition are important because they have major effects on the performance of the YSZ electrode (Ulmer, 1984).

The system has been tested for both precision and durability in experiments on NaCl–HCl solutions at temperatures above 300 °C using the flow-through YSZ electrode and a flow-through hydrogen (Pt) electrode in a configuration comparable to the hydrogen electrode concentration cell technology developed some years ago by Mesmer et al. (1970) with later improvements by Mesmer et al. (1995) and Wesolowski et al. (1995). The utility of the system is favored by its fast pH response, particularly at temperatures above about 200 °C (Niedrach, 1980a; Hettiarachchi and Macdonald, 1984), with the rate of response apparently being limited by the rate of mixing of solutions as they are pumped into the cell.

## 2. Potentiometric measurements

### 2.1. Recent designs of pH sensors

For pH measurements above 300 °C, the general characteristics required of the sensors are: (1) resistance to chemical degradation; (2) tolerance of thermal and pressure (mechanical) stress; (3) suitability for calibration using standard solutions; and (4) establishing of stable potentials that can be resolved within a few millivolts.

The use of Pt electrodes in hydrogen concentration cells and $Pd_xH|H^+$ systems for high-temperature pH measurement was an early development (Mesmer et al., 1970; Dobson, 1972; Sweeton et al., 1973; Macdonald et al., 1973a,b, 1980; Macdonald and Owen, 1973; Tsuruta and Macdonald, 1981). In particular, concentration cells employing $H_2-Pt$ electrodes were employed by Mesmer et al. (1970, 1995), Mesmer and Holmes (1992), Sweeton et al. (1973), and Wesolowski et al. (1995) to measure a large number of thermodynamic constants over a wide range of temperatures up to 300 °C. Macdonald et al. (1973a,b) and Macdonald and Owen (1973) used a similar cell to measure $K_w$, to investigate the hydrolysis of $Al^{3+}$ and the precipitation of boehmite ($\gamma$-AlOOH), and to derive transport numbers for $H^+$ and $Cl^-$ in aqueous HCl solutions at temperatures up to 200 °C.

Other types of high-temperature pH-measuring methods have been explored. For example, glass electrodes have been used to measure pH up to 254 °C (Kriksunov and Macdonald, 1995). The $W|WO_3$ electrode has also been explored (Dobson et al., 1976), with some measurements being reported at temperatures up to 550 °C (Kriksunov et al., 1994). However, both of these systems are secondary electrodes, which require calibration with a suitable pH reference solution ("buffer"). Until well-defined pH buffers for use at temperatures above about 300 °C are developed, secondary pH electrodes cannot be used for accurate pH measurements at high subcritical and at supercritical temperatures. Nevertheless, the simplicity and ruggedness afforded by metal oxide electrodes render them attractive, particularly for monitoring purposes where high accuracy or precision is not required.

Potentiometric sensors based on oxygen-ion conducting ceramics, such as yttria-stabilized zirconia (YSZ), were originally described by Niedrach (1980a,b, 1981, 1982, 1984), and were later explored by Tsuruta and Macdonald (1982), Niedrach and Stoddard (1984), Danielson et al. (1985a,b), and Bourcier et al., (1987). One system developed by Niedrach and co-workers employed a Cu/CuO internal reference element to yield a sensor that can be formally represented as $Cu|CuO|ZrO_2(Y_2O_3)|H^+$, $H_2O$, while another employed a $Ag|AgCl|NaCl$ internal element at the operating temperature of the cell (up

to 285 °C). The latter system was found to be Nernstian at 25 and at 95 °C, as determined by comparing the response against that of an glass electrode, and at 285 °C by comparing the response against that of an oxygen electrode. The response was found to be rapid at the higher temperature and appeared to be determined by the rate of mixing of the solutions in the high-pressure cell. No redox response to changes in oxygen fugacity was observed. While other workers (Bourcier et al., 1987) did see a supposed redox response upon injection of $H_2O_2$ or with air saturated solutions, the interpretation of those observations is that they were rather corrosion-induced responses. Although the pH-sensing capabilities of this electrode were well recognized by Niedrach (1984) and Niedrach and Stoddard (1984), it was developed primarily as a reference electrode for use in water-cooled nuclear reactors. Tsuruta and Macdonald (1982) also employed a Ag|AgCl, KCl internal element, but they located the reference element at the cold end of the internal electrolyte junction, so as to prevent thermal hydrolysis of AgCl. Potentials were measured against an external pressure-balanced reference electrode (EPBRE) having an identical internal solution subjected to the same temperature gradient. In this manner, the thermal liquid-junction potentials of both electrodes should cancel, thereby eliminating the largest uncertainty associated with the EPBRE and hence allowing appropriate pH measurements to be made. Nernstian behavior was demonstrated at 250 and 275 °C, with some deviations in dilute sulfuric acid solutions. Provided that the internal reference solution in the YSZ sensor was sufficiently well buffered, this pH sensor was found to be highly stable at 250 °C. The lack of Nernstian behavior at lower temperatures (cf. Niedrach, 1980a,b) was traced to an abnormally high membrane impedance. This configuration, while highly promising for making pH measurements of high precision, was subsequently abandoned in favor of the simpler YSZ sensors based on metal/metal oxide internal couples.

### 2.1.1. Electrode defects

Many of the early attempts to use YSZ membranes as pH-sensing electrodes suffered from poor electrical characteristics of the ceramic, as indicated above. For example, Bourcier et al. (1987) measured pH at temperatures up to 275 °C. They found that a small subset of the YSZ tubes from some manufacturers gave a Nernstian response and that the cell potentials, measured with the YSZ against a reference electrode, drifted in long-term tests of several hundred hours. They further investigated this problem by focusing on the microstructure and composition of both responsive and non-sensing YSZ tubes and concluded that microstructural and microcompositional factors were of great importance in determining the performance of the electrode.

Hettiarachchi and Macdonald (1984) used Hg/HgO as the internal couple in YSZ sensors that were evaluated at temperatures ranging from 175 to 275 °C in a variety of solutions having pH values from 2.30 to 9.32 at 275 °C. The ceramic tubes used in that study were obtained from a different supplier than were those employed by Tsuruta and Macdonald (1982) and were prepared with (ostensibly) no additions of "sintering aids." Nernstian response was observed at all temperatures (175 to 275 °C), as determined by plotting the potential of the YSZ sensor vs. an EPBRE (Ag|AgCl, 0.1 mol kg$^{-1}$ KCl) against that of a hydrogen sensor (Pt, $H_2/H^+$) vs. that of the same EPBRE as the pH was changed over a wide range, with the measurements being performed simultaneously. In this configuration, any uncertainty in the potential of the EPBRE (e.g., those due to the thermal and isothermal liquid-junction potentials) or in the pH of the solution (due to corrosion) cancels and Tsuruta and Macdonald were then able to explore the performance of the YSZ sensor relative to that of the hydrogen electrode. The slope of the correlation was found to vary from 1.018 (175 °C) to 0.997 (275 °C), with an average value of 1.006 (i.e., a 0.6% deviation), while the regression coefficient varied from 0.998 (250 °C) to 0.999 (225 °C). The average deviation of the experimental points from the correlation lines is estimated to be about 10 mV, corresponding to an uncertainty of 0.1 pH units at the highest temperature.

In a later study, Hettiarachchi et al. (1985) further explored the $Hg|HgO|ZrO_2(Y_2O_3)$ electrode, and their correlations, with simultaneously measured potentials from a hydrogen sensor at temperatures ranging from 125 to 275 °C, displayed a level of precision comparable to that noted above. However, when the potential was measured against an EPBRE and then plotted as a function of pH (calculated from the system composition), much lower precision was evident. Deviations of

up to $\pm 50$ mV, corresponding to about $\pm 0.5$ pH units, were evident in acid solutions, although better precision was obtained in alkaline solutions at 275 °C. The poor performance of the sensor in acidic solutions is due primarily to corrosion, which produces a pH that is different from that calculated from the assumed solution model. This is not an issue for the YSZ electrode vs. (Pt) $H_2/H^+$ correlation, because both electrodes experience the same pH and hence any deviation in pH causes identical shifts in the potentials of the two electrodes. This study also demonstrated that the potential of the YSZ sensor is independent of the oxygen fugacity ($f_{O_2}$), hydrogen fugacity ($f_{H_2}$), chloride concentration and sulfide concentration. The lack of a dependence of the YSZ electrode potential on $f_{O_2}$ and $f_{H_2}$ is particularly important, because it demonstrates an independence of redox potential, which is important in geochemical and corrosion studies. Although work by Niedrach (1980a,b) and Hettiarachchi et al. (1985) demonstrated the lack of a redox response, some concern still exists for the success of $ZrO_2$-pH sensors in geothermal systems as will be discussed in a later section.

The lack of dependencies of the YSZ potential on aqueous $Cl^-$ and $HS^-$ anions implies that neither of these species interferes with the potential-determining equilibrium at the ceramic/solution interface. Bourcier et al. (1987) also discovered that $F^-$ ion was not an interfering species for $ZrO_2$-pH sensors despite the interesting fact that $OH^-$ and $F^-$ have the same ionic radii (1.33 Å).

In another use of YSZ electrodes, Macdonald et al. (1988, 1992), and Hettiarachchi et al. (1985, 1992) explored the $Hg|HgO|YSZ|H^+$, $H_2O$ electrode as a pH sensor for measuring pH in high-temperature subcritical and supercritical aqueous systems. The potential was found to drift with time and the authors concluded that such errors are caused principally by the reference electrode and corrosion of the wetted surfaces of the apparatus and hence to changes in the pH of the solution.

The YSZ electrode was also used for a series of pH and hydrogen concentration measurements by Ding and Seyfried (1996a). They measured the pH of a NaCl-bearing fluid at 400 °C and 40 MPa, with a precision of $\pm 0.1$ pH units. As noted above, they also used YSZ electrodes to measure the concentration of dissolved hydrogen in supercritical aqueous

solutions at 400 °C and 40 MPa (Ding and Seyfried, 1995, 1996b). Similarly, Eklund et al. (1997) evaluated the Henry's Law constant for hydrogen up to 450 °C, and they demonstrated the Nernstian behavior of the YSZ sensor at temperatures well above the critical temperature of water.

### 2.1.2. Electrode mechanisms

The mechanisms and thermodynamics of operation of the YSZ pH sensor have been explored by Tsuruta and Macdonald (1982), Bourcier et al. (1987), and by Macdonald et al. (1988). In the work of Tsuruta and Macdonald (1982), a buffered aqueous reference element was employed, as noted above, and the potential determining process on both sides of the membrane was attributed to the equilibrium

$$H_2O \leftrightarrow 2H^+(aq) + O^{2-}(YSZ) \tag{3}$$

which gives the membrane potential, $\Delta\phi_m$, as

$$\Delta\phi_m = (2.303RT/F)(pH_1 - pH_2) \\ + (\mu_{H_2O,1} - \mu_{H_2O,2}) \tag{4}$$

provided that the membrane is uniform in composition and is at equilibrium. In this expression, $\mu_{H_2O,1}$ and $\mu_{H_2O,2}$ are the chemical potentials of water on the outside and inside, respectively, of the membrane. Because these quantities are only weakly dependent on composition for dilute solutions, the membrane and hence sensor potential should be Nernstian.

The thermodynamics of YSZ sensors containing metal/metal oxide internal reference elements, that is $M|MO_x|ZrO_2(Y_2O_3)|H^+,H_2O$, has been further analyzed in detail by Macdonald et al. (1988, 1992) and Lvov et al. (1995). Using standard notation for oxygen vacancies, $V_{\ddot{O}}$, they attributed the potential-determining equilibria at the solution side and at the internal reference element side of the membrane to

$$V_{\ddot{O}} + H_2O \leftrightarrow O_O + 2H^+ \tag{5}$$

and

$$MO_x + xV_{\ddot{O}} + 2xe^- \leftrightarrow M + xO_O \tag{6}$$
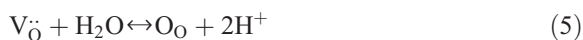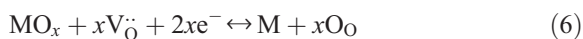
respectively. Provided that the membrane is in equilibrium with respect to the oxygen sublattice (i.e., the oxygen vacancy activity is constant throughout the ceramic) and that the measurement is carried out potentiometrically (zero current through the mem-

brane), the sensor potential is determined by the equilibrium

$$MO_x + 2xH^+ + 2xe^- \leftrightarrow M + xH_2O \qquad (7)$$

for which the Nernst equation is

$$E = E^0_{M/MO_x} - \left(\frac{2.303RT}{2F}\right)\log(a_{H_2O})$$
$$- \left(\frac{2.303RT}{F}\right)pH \qquad (8)$$

where $E^o_{M/MO_x}$ is the standard potential of the $M/MO_x$ couple relative to the reference state of $H_2$ (g, T, 1 bar) and $a_{H_2}O$ is the activity of water on the solution side of the membrane. The form of Eq. (8) is important for three reasons: (1) the potential of the YSZ sensor should be Nernstian with respect to pH, (2) the accuracy significantly depends on the choice of the metal/metal oxide redox couple, and (3) no property of the ceramic membrane appears in any of the terms. This latter condition arises from assuming that the YSZ is at equilibrium with respect to its oxygen vacancy structure. Hg|HgO is a well-characterized metal/metal oxide redox couple in electrochemistry, in terms of reversibility and thermodynamics, and this electrochemical system has been found (Macdonald et al., 1988, 1992) to be a reliable internal reference element. However, the Hg|HgO couple could have a disadvantage at temperatures above 350 °C due to vaporization of Hg(l). Others in geosciences have found the Cu|CuO redox couple also an advantageous and reliable system to be used at higher temperatures (Bourcier et al., 1987; Manna, 2002). Finally, after correcting for the activity of water, the sensor potential should extrapolate to $E^o_{Hg/HgO}$ for each temperature. This was shown to be the case in the work of Macdonald et al. (1988), Lvov et al. (1995), and in the studies of Eklund et al. (1997). The agreement between Eq. (8) and experiment demonstrates the correctness of the potential-determining equilibria represented by Reactions (5) and (6) above. Finally, the form of Eq. (8) demonstrates that the YSZ sensor can be a pH primary electrode, because all of the quantities on the right hand side (except pH) are known (Hettiarachchi et al., 1985; Macdonald et al., 1988; Eklund et al., 1997). This is a most important property, because it

means that, in principle, the YSZ sensor does not require calibration, provided that a thermodynamically well-behaved reference electrode is available.

## 2.2. Reference electrodes

While the EPBRE can be made to perform satisfactorily, given sufficient care, as shown by the results of Hettiarachchi et al. (1985) for alkaline systems, it is generally unsuitable, and was never intended for routine, high precision pH measurements. Under normal operation (i.e., without provision for countering thermal diffusion), the EPBRE can be expected to provide a reference voltage accuracy of no better than ± 10 to 30 mV, corresponding to an uncertainty in the measured pH at 275 °C of about 0.1 to 0.3 pH units. While this level of precision is suitable for many monitoring applications, it is not suitable for fundamental studies. Two approaches have been adopted in attempting to improve the precision of the reference electrode. Thus, Pang et al. (1993) devised a system in which the test solution and a buffer solution were pumped alternately through a cell containing a YSZ pH sensor and an EPBRE, with the buffer cycle being used to calibrate the reference electrode by using the known potential of the YSZ electrode. The calibrated reference electrode potential was then used for the measurement of the YSZ electrode potential, and hence for the calculation of the pH of the test solution. Under general conditions, this approach could yield a precision in the measured pH of ± 0.1, assuming no uncertainty in the temperature at the electrode tip. However, the technique relies upon the availability of a suitable buffer, which is a major problem for temperatures greater than about 300 °C.

Lvov and Macdonald (1997), Lvov et al. (1998a,b, 1999) and Lvov and Zhou (1998) developed a "flow-through" EPBRE, which employs a flowing solution in the non-isothermal bridge to suppress any tendency for concentration gradients to develop from thermal diffusion and hence to maintain the system in the Soret initial state. A means for maintaining the reference electrode in this state was also embodied in the original EPBRE. In that case, a flexible compartment containing the non-isothermal bridge allowed periodic volume pulsation in response to pressure pulses from the positive displacement pump to minimize the thermal diffusion and the system would be

maintained in the Soret initial state (Macdonald et al., 1979b). However, it proved to be very difficult to determine when the intensity of pulsation was just sufficient to maintain the initial Soret state. If the intensity is too large, excessive mixing occurs between the reference electrode internal and external solutions, thereby causing the reference potential to drift, because of changing solution composition. On the other hand, the flow-through approach is proving to be very successful, albeit at a cost in complexity, because of the need to have an additional flow circuit. Nevertheless, the quest for a precise reference electrode for use under laboratory conditions has now been largely achieved.
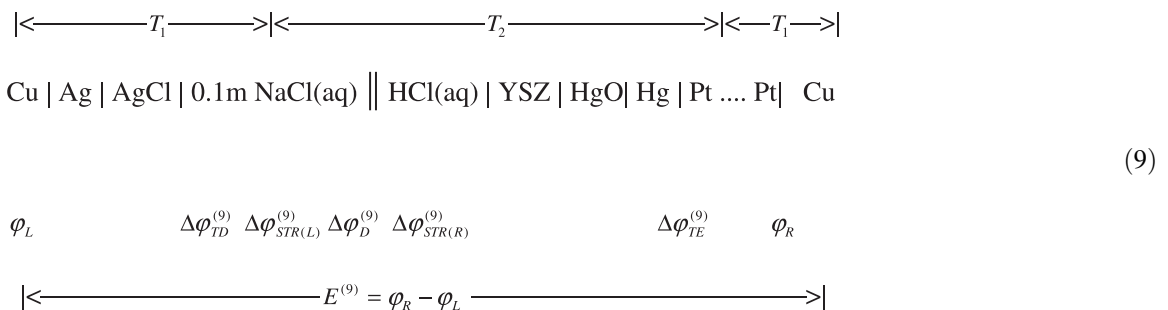
As noted above, the principal problem in developing a suitable external reference electrode was a resolution of the thermal liquid-junction potential issue, which has its roots in the Soret effect (Macdonald et al., 1979a,b; Lvov et al., 1995; Lvov and Macdonald, 1996). A major advance in addressing this problem was the development of the flow-through reference electrode (FTRE) (Lvov and Zhou, 1998; Lvov et al., 1998a,b). The unique advantage of this reference electrode is that the reference solution flows through the electrode at constant velocity in a constant geometry. Therefore, the concentration of solution across the thermal liquid junction remains constant and any uncertainty in the thermal liquid-junction potential can be eliminated for measurements at given temperature and pressure. In tests of this reference electrode, Lvov et al. (1998a,b) used a thermocell, which has a Pt($H_2$) electrode as a pH sensor for potential measurements up to about 400 °C and to 33.8 MPa. Dilute HCl and NaOH aqueous solutions have been used in these first studies. Recent improvements (Lvov and Zhou, 1998; Lvov et al., 1999) allow

potential measurements to be made to a precision of 3–5 mV and pH to $\pm 0.05$ at temperatures up to 400 °C.

### 2.3. Construction of the high-temperature test module

The cell used for electrode testing is shown in Fig. 1, and is much evolved from an earlier version described in Lvov and Zhou (1998) and Lvov et al. (1999). The body is of a corrosion-resistant alloy, Hasteloy-B, and has four ports into which different components can be sealed for use at high pressures and temperatures. The components include a flow-through reference electrode, a flow-through $H_2$–Pt electrode, a flow-through yttria-stabilized zirconia electrode and a thermocouple. The design has a four-way, once-through, pumped fluid circulation through the electrodes at rates faster than thermal diffusion, so that no concentration gradients result from the Soret effect. Only the sensing portion of the system needs to be, and is, maintained at controlled temperatures and pressures. The purity and concentration of the solutions were maintained by relatively rapid flow. Therefore, contamination of an individual packet of test solution is minimized by this flow. Because the low temperature input flow is in contact only with glass, Teflon, and PEEK (polyether ether ketone) tubes (which have high corrosion-resistance) and during its high-temperature outflow only with zirconia and platinum, greater control is achieved on the solution composition at the sensing portion of the system. Use of these particular materials is a crucial requirement for accurate pH measurements by this system.

The electrochemical system of Fig. 1 is a thermocell with the top of the electrodes at ambient temperatures and the bottom at high, experimental temperatures, where its potential is established by:

$$|\!\!\longleftarrow\!\!-T_1\!-\!\!\longrightarrow\!|\!\!\longleftarrow\!\!-T_2\!\!\longrightarrow\!|\!\!\longleftarrow\!-T_1\!-\!\!\longrightarrow\!|$$

$$\text{Cu} \,|\, \text{Ag} \,|\, \text{AgCl} \,|\, 0.1\text{m NaCl(aq)} \,\|\, \text{HCl(aq)} \,|\, \text{YSZ} \,|\, \text{HgO}|\, \text{Hg} \,|\, \text{Pt} .... \text{Pt}| \ \ \text{Cu}$$

$$(9)$$

$$\varphi_L \qquad\qquad \Delta\varphi_{TD}^{(9)} \ \ \Delta\varphi_{STR(L)}^{(9)} \ \Delta\varphi_D^{(9)} \ \ \Delta\varphi_{STR(R)}^{(9)} \qquad\qquad \Delta\varphi_{TE}^{(9)} \qquad \varphi_R$$

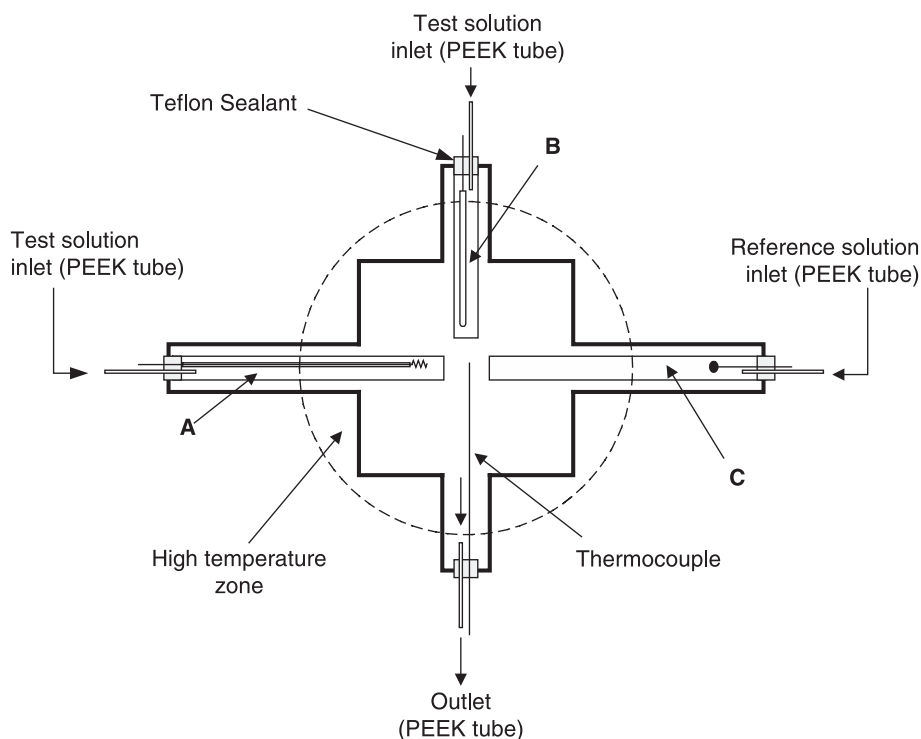$$|\!\!\longleftarrow\!\!\longrightarrow E^{(9)} = \varphi_R - \varphi_L \longrightarrow\!|$$

Fig. 1. Schematic of a high-temperature electrochemical module made of Hasteloy-B alloy, designed for comparative testing of YSZ pH-sensing electrodes and other electrodes. (A) Flow-through $H_2$–Pt electrode, (B) flow-through YSZ pH-sensing electrode, (C) flow-through external reference electrode. Design of YSZ pH-sensing electrode B is shown in Fig. 2. Design of flow-through $H_2$–Pt, A, and flow-through external reference electrode C are found in the works of Lvov et al. (1998a,b, 1999), and Lvov and Zhou (1998). PEEK tubes are made of the polyethylethylketone polymer (Alltech). Three high-pressure chromatography pumps have been used in running this module.

where $E^{(9)}$ is the electromotive force (emf) of the thermocell (9), $\varphi_L$ and $\varphi_R$ are the electrostatic potentials of the left and right terminals, respectively, at ambient temperature $T_1$, and $T_2$ is an elevated temperature that is higher than $T_1$. Note that Cu in the schematic (9) represents the wires to connect the terminals of the system and an electrometer. The value $E^{(9)}$ can be expressed as:

$$
\begin{aligned}
E^{(9)} = \frac{1}{F} & \left[ \mu_{H^+}(T_2) + \mu_{Cl^-}(T_1) - \frac{1}{2}\mu_{H_2O}(T_2) \right. \\
& + \frac{1}{2}\mu_{HgO}(T_2) - \mu_{AgCl}(T_1) - \frac{1}{2}\mu_{Hg}(T_2) \\
& \left. + \mu_{Ag}(T_1) \right] + \Delta\varphi^{(9)}_{TE} + \Delta\varphi^{(9)}_{D} + \Delta\varphi^{(9)}_{STR(R)} \\
& + \Delta\varphi^{(9)}_{STR(L)} + \Delta\varphi^{(9)}_{TD}
\end{aligned}
\tag{10}
$$

where $\mu_i(T_1)$ and $\mu_i(T_2)$ are the chemical potentials of the $i$th species at temperature $T_1$ and $T_2$, respectively. In Eq. (10), $\Delta\varphi^{(9)}_{TE}$, $\Delta\varphi^{(9)}_{D}$, $\Delta\varphi^{(9)}_{STR}$, and $\Delta\varphi^{(9)}_{TD}$ are respectively the thermoelectric, diffusion, streaming and thermal diffusion potentials which have been discussed in detail elsewhere (Lvov and Zhou, 1998; Lvov et al., 1999). It is assumed that the oxygen vacancy structure in the YSZ ceramic membrane is in equilibrium and that the electrochemical potential of an oxygen vacancy on the internal reference side of the membrane is the same as that on the test environment side of the membrane.

Because the theory and the basic design of the flow-through reference and Pt($H_2$) electrodes have been described (Lvov and Macdonald, 1996; Lvov et al., 1998a,b, 1999), only the structures of the principal flow-through YSZ sensor will be discussed below.

## 2.4. Design of the flow-through yttria-stabilized zirconia pH sensor

The configuration of the YSZ electrode is illustrated in Fig. 2 (Zhou et al., 2001, 2003). Crucial to this design is a dual sealing system. In particular, the impermeable YSZ tube (8 mol% $Y_2O_3$, from Coors Ceramic) is 0.625 cm in diameter, 0.076 cm in wall thickness, and 25 cm in length. Hg|HgO paste was made from Hg and synthetic HgO (99.998% pure from AESAR) and sealed in the bottom part of the tube with $ZrO_2$ sand (Tam Ceramics) and with 904 zirconia ultra high-temper-ature ceramic cement (Cotronics) inserted and baked to 200 °C. The top of the zirconia cement column was sealed with Chemgrip epoxy adhesive glue (Norton Performance Plastics). Previously, YSZ pH electrodes were installed in the high-pressure systems with a part of the ceramic tube separating high-pressure and high-temperature fluid from the external environment (e.g., Tsuruta and Macdonald, 1981; Bourcier et al., 1987; Eklund et al., 1997). In the current design, the entire ceramic tube is within the metal-gland-sealed, high-pressure volume with no ceramic wall serving as an external pressure boundary. This design of the YSZ pH sensor sig-
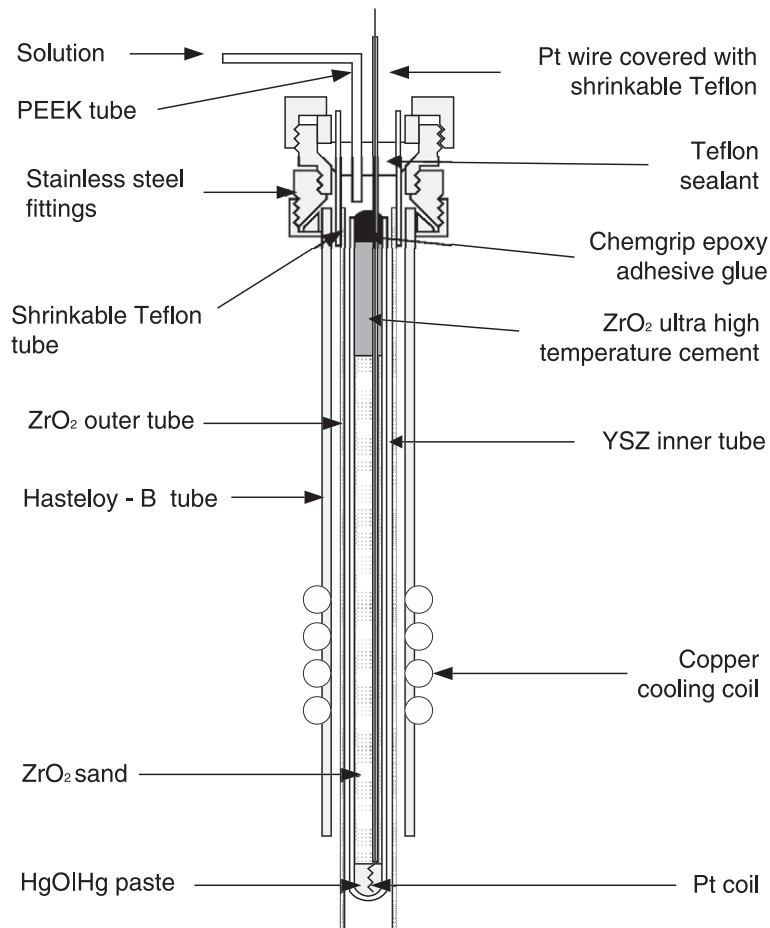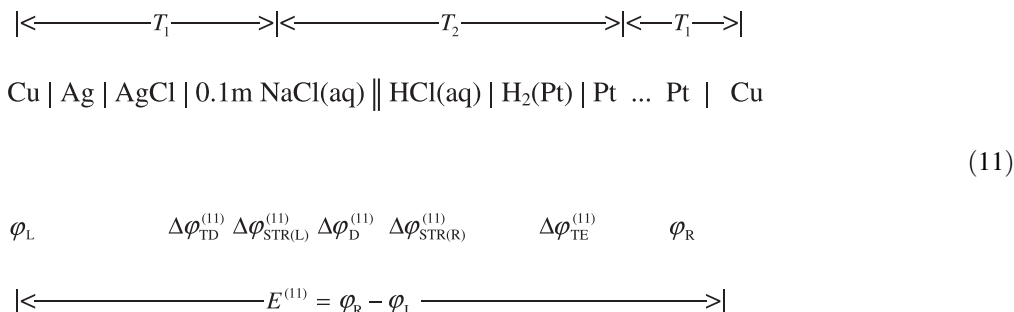


Fig. 2. Design of the flow-through, YSZ, pH-sensing electrode. Stainless steel fittings consist of a transducer gland (Connax Buffalo Technologies) with a Teflon sealant (Du Pont).

nificantly increases possible applications and safety of the high-temperature pH measurements. However, it should be mentioned that relatively short operational time (1 to 3 months) of the YSZ pH sensor was observed in high-temperature aqueous solutions due to possible dissolution of the interstitial materials used for making the YSZ membranes.

*2.5. Experimental procedures using the flow-through thermocell with hydrogen–platinum and reference electrodes*

Another comparative thermocell again is designed to use across the same temperature gradient as the YSZ electrode in the test module (Fig. 1):

$$|\!\!\longleftarrow\!\!-T_1\!\!-\!\!\longrightarrow\!\!|\!\!\longleftarrow\!\!-\!\!-\!\!T_2\!\!-\!\!-\!\!-\!\!\longrightarrow\!\!|\!\!\longleftarrow\!\!-T_1\!\!-\!\!\longrightarrow\!\!|$$

$$\text{Cu} \mid \text{Ag} \mid \text{AgCl} \mid 0.1\text{m NaCl(aq)} \parallel \text{HCl(aq)} \mid \text{H}_2(\text{Pt}) \mid \text{Pt} \; \dots \; \text{Pt} \mid \text{Cu}$$

(11)

$$\varphi_L \qquad\qquad \Delta\varphi_{TD}^{(11)}\; \Delta\varphi_{STR(L)}^{(11)}\; \Delta\varphi_{D}^{(11)}\; \Delta\varphi_{STR(R)}^{(11)} \qquad \Delta\varphi_{TE}^{(11)} \qquad \varphi_R$$

$$|\!\!\longleftarrow\!\!-\!\!-\!\!-\!\!-\!\!-\!\!-\!\!-\!\!-\!\! E^{(11)} = \varphi_R - \varphi_L \;-\!\!-\!\!-\!\!-\!\!-\!\!-\!\!-\!\!-\!\!\longrightarrow\!\!|$$

where the parameters are the same as for thermocell (9). Because the flow-through process constantly renews the solutions, the $E^{(11)}$ value can be expressed as (Lvov and Zhou, 1998; Lvov et al., 1999):

$$E^{(11)} = \frac{1}{F}\left[\mu_{H^+}(T_2) + \mu_{Cl^-}(T_1) - \frac{1}{2}\mu_{H_2}(T_2)\right.$$
$$\left. - \mu_{AgCl}(T_1) + \mu_{Ag}(T_1)\right] + \Delta\varphi_{TE}^{(11)} + \Delta\varphi_{D}^{(11)}$$
$$+ \Delta\varphi_{STR(R)}^{(11)} + \Delta\varphi_{STR(L)}^{(11)} + \Delta\varphi_{TD}^{(11)} \qquad (12)$$

where the parameters are the same as defined for Eq. (10). The evaluation of the thermoelectric ($\Delta\varphi_{TE}^{(11)}$), diffusion ($\Delta\varphi_{D}^{(11)}$), streaming ($\Delta\varphi_{STR}^{(11)}$) and thermal diffusion ($\Delta\varphi_{TD}^{(11)}$) potentials, has been described elsewhere (Lvov et al., 1999).

Experimental measurements with the module of Fig. 1 were made by using simultaneously the flow-through YSZ pH-sensing electrode (B), the flow-through external reference electrode (C) and a flow-through $H_2$–Pt electrode (A). The first sets of data were obtained at temperatures of 320 and 350 °C, and pressure of 23.0 and 24.8 MPa, respectively. The reference solution of the flow-through reference electrode was 0.100 mol $kg^{-1}$ NaCl. Test solutions could be directed from a T-junction either through the $H_2$–Pt electrode or through the YSZ electrode. This

allowed both the compositions of the solutions and the flow rates through the two electrodes alternatively to be the same. The reference electrode solution was de-aerated using helium while the test solution was purged with ultra-high purity hydrogen (99.99%).

*2.6. Experimental results*

The difference between the potentials of the flow-through $H_2$–Pt electrode, $E^{(11)}$ and the flow-through YSZ electrode, $E^{(9)}$, from Eqs. (10) and (12) is:

$$E^{(11)} - E^{(9)} = \frac{1}{2F}\left[\mu_{H_2O}(T_2) - \mu_{H_2}(T_2) + \mu_{Hg}(T_2)\right.$$
$$- \mu_{HgO}(T_2)\Big] + \left[\left(\Delta\varphi_{TE}^{(11)} - \Delta\varphi_{TE}^{(9)}\right)\right.$$
$$+ \left(\Delta\varphi_{D}^{(11)} - \Delta\varphi_{D}^{(9)}\right) + \left(\Delta\varphi_{STR(R)}^{(11)}\right.$$
$$- \Delta\varphi_{STR(R)}^{(9)}\Big) + \left(\Delta\varphi_{STR(L)}^{(11)}\right.$$
$$- \Delta\varphi_{STR(L)}^{(9)}\Big) + \left(\Delta\varphi_{TD}^{(11)} - \Delta\varphi_{TD}^{(9)}\right)\Big],$$

(13)

Because the temperature, pressure, flow rate, and solution composition were the same in the flow-through YSZ and $H_2$–Pt electrodes, the terms inside the second square brackets were negligible (Lvov et al.,

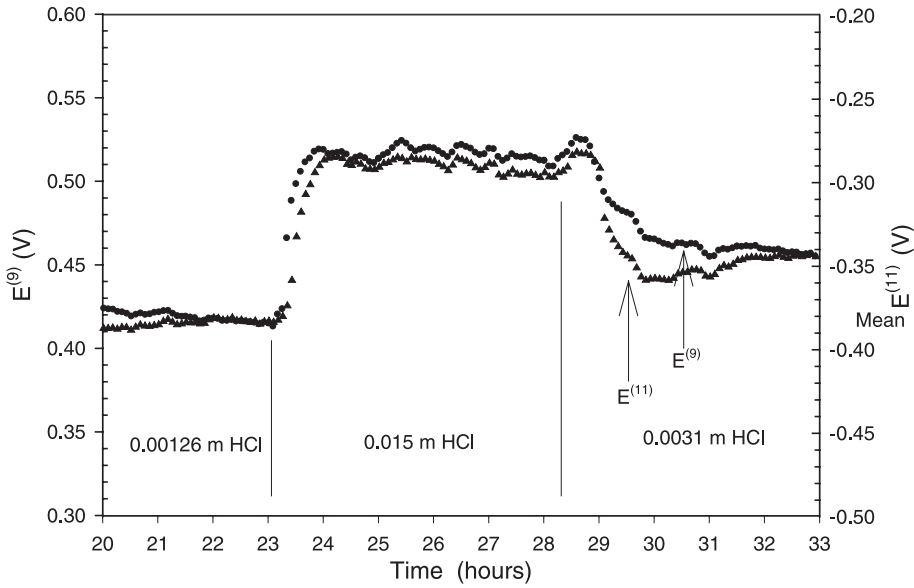Fig. 3. Potentials of the YSZ, pH-sensing electrode and of the $H_2$–Pt electrode vs. time at 320 °C, 23.0 MPa, and flow rates of 0.25 ml min$^{-1}$. $E^{(9)}$, $E^{(11)}$ are, respectively, the potentials of the flow-through, YSZ, pH-sensing electrode and the flow-through, $H_2$–Pt electrode vs. the flow-through external reference electrode (Ag/AgCl).

1999). All terms inside the first square brackets are independent of the activity of $H^+$. Thus, under constant temperature, pressure, flow rate, and dissolved hydro-

gen concentration, the difference between the potentials of the flow-through $H_2$–Pt and the flow-through YSZ electrodes should be constant and independent of
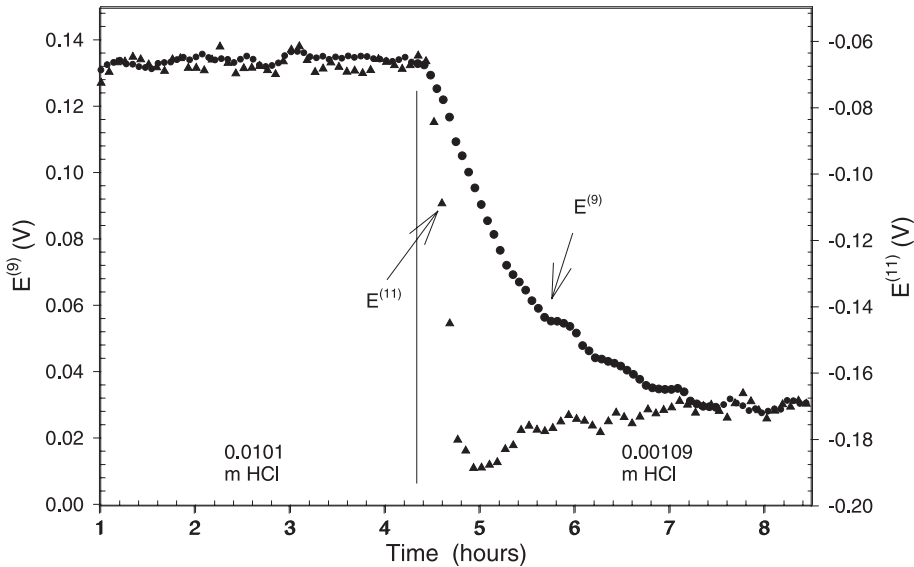


Fig. 4. Measured potentials of the YSZ, flow-through pH-sensing electrode, $E^{(9)}$, and the flow-through $H_2$–Pt electrode, $E^{(11)}$, recorded during experiment at 350 °C, 24.8 MPa, and a flow rate of 0.5 ml min$^{-1}$. Time of response of the YSZ electrode to pH changes is about as fast as that of the $H_2$–Pt electrode.

the activity of $H^+$. This deduction is certified by the experimental data of Figs. 3 and 4, where the potential differences due to pH changes for both electrodes are in agreement within less than 5 mV. Because the uncertainty in pH measurements by the flow-through $H_2$–Pt electrode vs. the flow-through external reference electrode has been shown to be $\pm 0.05$ pH unit from 25 to 400 °C (Lvov et al., 1999), the precision of the flow-through YSZ vs. the flow-through external reference electrode for pH measurements is about the same as that of the flow-through $H_2$–Pt electrode vs. the flow-through external reference electrode. Therefore, above 300 °C, the precision of the flow-thorough YSZ electrode has been established to be 5 mV.

The rate of response of the YSZ electrode can be inferred from the time asymmetric data of Fig. 3. When a dilute (0.00126 mol $kg^{-1}$ HCl) solution was replaced by a concentrated (0.015 mol $kg^{-1}$ HCl) solution, the potentials became stable after only about 90 min. However, when the concentrated solution was replaced by a more dilute (0.0031 mol $kg^{-1}$ HCl) solution, the potential became stable only after 3–4 h (Fig. 3). Simple calculations show that at a flow rate of 0.5 ml $min^{-1}$, the fluid residence time in a 30 $cm^3$ cell is about 60 min. Even assuming complete mixing, more than 95% of initial fluid will be exchanged within 3 h. As can be seen from Figs. 3 and 4, the experimental data are consistent with our calculations of the replacement time so mixing apparently limits the equilibration time of the electrode potential. Evidently,

the response of the YSZ electrode to pH changes is about as fast as that of the hydrogen electrode.

The similar response time and potential change of the YSZ and $H_2$–Pt electrodes clearly confirm that both electrodes are identical with respect to their response to the activity of $H^+$. Therefore, both electrodes should be thermodynamically reversible and can be used for highly accurate pH measurements at temperatures above 300 °C.

To confirm the accuracy and Nernstian behavior of the flow-through YSZ electrode, we have measured the association constant of HCl(aq) at temperatures 320 °C (23.0 MPa) and 350 °C (23.0 MPa). Our method for deriving the association constant is presented elsewhere (Lvov et al., 2000a). Briefly, we measured the potentials of thermocell (9) for two HCl(aq) solutions with concentrations between 0.01 and 0.001 mol $kg^{-1}$ over a wide range of flow rates from 0.2 to 0.8 ml $min^{-1}$. The difference in the potentials was a linear function of the flow rate (Fig. 5) as was found in the past (Lvov et al., 1999). At zero flow rate, the difference, $\Delta E_{1,2}$, was evaluated by extrapolation. $\Delta E_{1,2}$ is related to the activity of $H^+$ by:

$$\Delta E_{1,2} = E_1 - E_2 = \frac{RT}{F} \ln\left\{\frac{[H^+]_1 \gamma_1}{[H^+]_2 \gamma_2}\right\} + (E_{d,1} - E_{d,2}) \tag{14}$$

where $E_1$ and $E_2$ are potentials of thermocell (9) for solution 1 ($\sim 0.01$ mol $kg^{-1}$ HCl) and solution 2
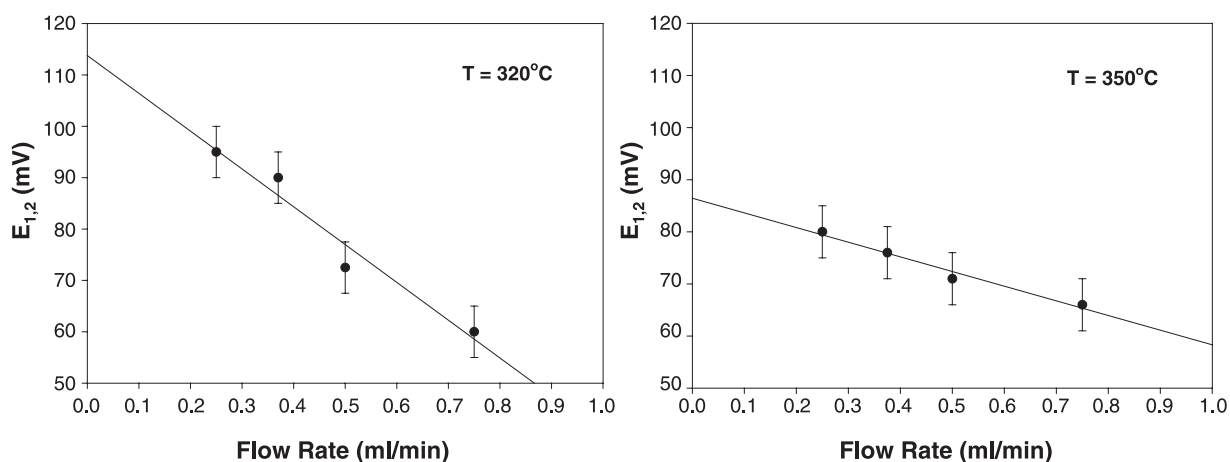


Fig. 5. The difference in potential between YSZ pH-sensing electrode and the flow-through external reference electrode (Ag/AgCl) as a function of flow rate at 320 °C (23.0 MPa) and 350 °C (23.0 MPa).

($\sim 0.001$ mol kg$^{-1}$ HCl), respectively; $[H^+]_1$ and $[H^+]_2$ are the concentrations of H$^+$ in solutions 1 and 2, respectively, $\gamma_1$ and $\gamma_2$ are the mean ionic activity coefficient of solutions 1 and 2, respectively, and $E_{d,1}$ and $E_{d,2}$ are the diffusion potentials. The concentration of H$^+$ is a function of the association constant ($K_{HCl}$) of aqueous HCl(aq) and is expressed as:

$$[H^+]_i = \frac{m_{HCl,i}}{K_{HCl}[H^+]_i\gamma_i^2 + 1} + \frac{K_w a_{H_2O}}{[H^+]_i\gamma_i^2} \qquad (15)$$

where $m_{HCl,i}$ is the analytical concentration of the $i$th HCl$_{(aq)}$ solution, $K_w$ is the water ionization constant (Bandura and Lvov, 2000), and $a_{H_2O}$ is the activity of water. For the dilute solutions, we used the activity coefficients and the activity of water, which can be evaluated with the second approximation of the Debye–Hückel theory:

$$\log\gamma_i = -\frac{z_i^2 A_m\sqrt{I_m}}{1 + B_m\mathring{a}\sqrt{I_m}} - \lg\left(1 + \frac{m_{tot}M_w}{1000}\right) \qquad (16)$$

$$\ln a_{H_2O} = \frac{m_{tot}M_w}{1000} \times \left\{1 - \frac{z_i^2 A_m}{1 + (B_m\mathring{a}\sqrt{I_m})^3}\right.$$
$$\times \left[(1 + B_m\mathring{a}\sqrt{I_m}) - 2\ln(1 + B_m\mathring{a}\sqrt{I_m})\right.$$
$$\left. - (1 + B_m\mathring{a}\sqrt{I_m})^{-1}\right] + \frac{1000}{m_{tot}M_w}$$
$$\left. \times \lg\left(1 + \frac{m_{tot}M_w}{1000}\right)\right\} \qquad (17)$$

where $z_i$ is the charge of the $i$th ion, $m_{tot}$ is the sum of the molalities of all the solute species in solution,

$M_w$ is the molar mass of water in g mol$^{-1}$, $I_m$ is the ionic strength of the solution on the molal concentration scale, $A_m$, $B_m$, and $\mathring{a}$ are the parameters of the Debye–Hückel theory. The value of $\mathring{a}$ was taken to be constant at 0.45 nm. The values of $A_m$ and $B_m$ were calculated using density and dielectric constant data for water taken from the Klein and Harvey (1996) computer code. The diffusion potentials were calculated using a recently developed approach based on the full integration method and compilation of high-temperature conductivity data (Zhou et al., 2000). By combining Eqs. (14)–(17), $K_{HCl}$ can be estimated if $\Delta E_{1,2}$ is obtained experimentally. The results of experimental measurements of $\Delta E_{1,2}$ as a function of flow rate at temperatures of 320 °C (23.0 MPa) and 350 °C (23.0 MPa) are presented in Fig. 5. The extrapolated $\Delta E_{1,2}$ values at zero flow rate are presented in Table 1. Also, the estimated association constants of HCl(aq) are given in Table 1. The errors for the observed p$K$ and pH values given in Table 1 were estimated using the standard deviation of $\Delta E_{1,2}$, which is 5.0 mV.

The accuracy of our $K_{HCl}$ value could be evaluated by comparison with data obtained by other methods, including conductivity, solubility, and calorimetric techniques. In Table 1, we present p$K = -\lg(K_{HCl})$ obtained here with the compilation, presented as an empirical analytical equation by Lvov et al. (2000b). Within the uncertainty of our experimental measurements, our data well agree with calculated values thereby supporting the validity of this measurement and the reliability of this potentiometric technique.

Table 1
Experimental data and calculated parameters for estimating the association constant of HCl, $K$ [p$K = -\lg K$]

| $T$, °C | $P$, MPa | Concentration of solution 1 (top) and solution 2 (bottom), mol kg$^{-1}$ | $E_{d,1} - E_{d,2}$, mV | $\Delta E_{1,2}$, mV | $\frac{RT}{F}\ln\left(\frac{\gamma_1}{\gamma_2}\right)$, mV | $\frac{RT}{F}\ln\left(\frac{[H^+]_1}{[H^+]_2}\right)$, mV | p$K$ of HCl, observed | p$K$ of HCl, calculated[a] | pH (observed) | |
|---|---|---|---|---|---|---|---|---|---|---|
| | | | | | | | | | Solution 1 | Solution 2 |
| 320 | 23.0 | 0.01500 0.00126 | 3.6 | $113.3 \pm 5.0$ | $-8.77$ | 118.47 | $-1.46 \pm 0.46$ | $-1.55 \pm 0.35$ | $2.02 \pm 0.05$ | $2.95 \pm 0.03$ |
| 350 | 24.8 | 0.01012 0.00109 | 3.7 | $93.4 \pm 5.0$ | $-7.40$ | 97.10 | $-2.35 \pm 0.25$ | $-2.39 \pm 0.35$ | $2.35 \pm 0.07$ | $3.08 \pm 0.03$ |

[a] Lvov et al. (2000b).

## 3. Discussion

### 3.1. Nernstian behavior

If the YSZ electrode is Nernstian, its response fits Eq. (8), here written for a Hg|HgO electrochemically sensitive couple as:

$$E = E^0_{HgO/Hg} + \frac{RT}{2F} \ln \frac{a^2_{H^+}}{a_{H_2O}} \qquad (18)$$

where $E$ is the electrode potential, $E^0_{HgO/Hg}$ is the standard electrode potential which was estimated over a wide range of temperatures (Hettiarachchi et al., 1985; Eklund et al., 1997), and $a_{H^+}$ is the activity of $H^+$(aq) ions to be determined in the pH measurements. To be specific, the characteristics, which are required for high quality pH measurements using the YSZ electrode include: (1) chemical durability, (2) phase stability, and (3) a constant and known charge carrier. In a review paper Gouma et al. (1998) concerning the microstructural characterization of sensors based on electronic ceramic materials, they state from a review of the literature: "Different fabrication methods are known to result in a variety of microstructures and varying response characteristics for a given sensor; there have been no systematic studies to identify an optimal processing technique. In large measure, this is because detailed characterization of the materials, including the relationships between microstructure and properties, is still lacking." For these reasons, we have focused much effort on the understanding of the $ZrO_2$-pH sensor behavior in relationship to the microstructure and other chemical properties of the ceramics involved.

It has long been recognized that the YSZ electrode can be used as a pH sensor (e.g., Niedrach, 1980a,b, 1981). In these papers, Niedrach used a $ZrO_2$ ceramic made in-house by the Lucalox® Division of General Electric who had the capacity to make ultra-pure $ZrO_2$ ceramics. While the exact composition was never revealed, it is believed that these ceramics were purer than those otherwise available in the commercial world. Niedrach did not directly demonstrate his sensors as a pH sensor at temperatures above 95 °C— only as a reference electrode. He did demonstrate its pH response indirectly at temperatures up to 285 °C by measuring the potential against an oxygen elec-

trode, which is not a very good reference system. Note that the effects of microstructure on the ceramic membrane properties are especially important because an alteration in microstructure can cause a change in the charge carrier. Constancy in Nernstian behavior over a wide temperature range implies that the YSZ electrode has had the same charge carrier.

### 3.2. Chemical durability

Although $ZrO_2$ and $Y_2O_3$ have low solubilities in water and strong acids, the useful life of manufactured YSZ tubes used in the current study may have been limited by leaching of them or of other oxide or silicate interstitial compounds. Unfortunately, the solubility of $ZrO_2$ and the yttria–zirconia solid solution are poorly known. From the data of Aja et al. (1995) and Shock et al. (1997) and neglecting the potentially important contributions of any complexing ligands except hydroxyl, the solubility of $ZrO_2$ at 25 °C, 0.1 MPa, and at 100, 200, and 300 °C, 50 MPa may be calculated. Results plotted in Fig. 6 suggest that the solubility of $ZrO_2$ is low in the pH range of common geothermal solutions, which are typically within 1 to 2 pH units of neutrality at fixed pressure and temperature (Kacandes and Grandstaff, 1989; Polster and Barnes, 1994). The calculations also indicate that, at low pH, with increasing temperature, the solubility of $ZrO_2$ decreases, making the $ZrO_2$ component of YSZ electrodes more resistant to acidic attack. However,
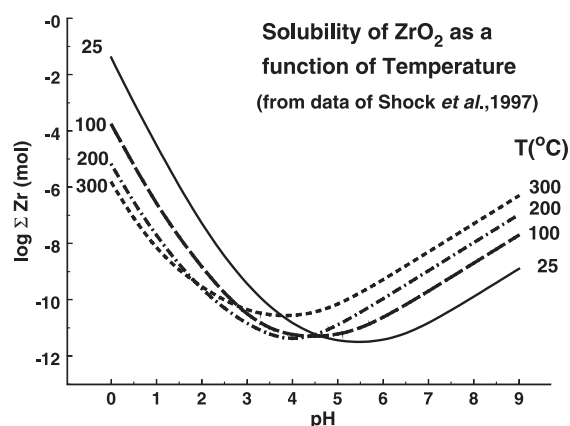


Fig. 6. The solubility of $ZrO_2$ ($\Sigma Zr = Zr^{4+} + Zr(OH)_n^{(+4-n)}$, for $1 < n < 5$) as a function of temperature (25 °C at 0.1 MPa, others at 50 MPa) based on thermodynamic values from Shock et al. (1997).

inter-granular oxide and silicate minerals and silicate glass present in some commercial YSZ tubes are comparatively vulnerable to acid solutions.

High-magnification scanning electron microscope (SEM) images of the texture within the wall of a commercial YSZ tube used in our experiments are presented in Figs. 7 and 8. Fig. 7a reveals an interstitial glass present in a randomly chosen planar section. The electron microprobe secondary electron image at a higher magnification (Fig. 7b) of the same ceramic shows that a glass phase is continuous in the two-dimensional view of the grain boundaries. The dihedral angles at each three-grain junction (Fig. 7b) reveal that the glass forms a three-dimensional continuum along the grain boundaries of the $ZrO_2$ ceramic (German, 1985). This grain boundary network glass, which may contribute to the bulk electrode conductivity (Badwal and Drennan, 1988), is a non-stoichiometric, anorthite-like glass with microprobe molar ratios of Si/Al = 1.50:1.60; Al/Ca = 0.64:0.70; and Si/Ca = 0.89:0.92.

The results of leaching the commercial YSZ tube in experiments with ∼ 0.001 to 0.01 molal HCl(aq) at 200–380 °C are shown in Fig. 8a. After several hundreds of hours, the glass phase at the grain boundaries has been leached to a depth of about 18% of the total wall thickness. Similarly, Fig. 8b shows analogous leaching of the same grain boundary phase after exposure to 10 mol $kg^{-1}$ HCl(aq) at 100 °C for 10 min. Handling of these samples (Fig. 8) reveals that the exposed surfaces of the YSZ have lost strength and, become chalky and very porous. Furthermore, Fig. 9 shows images of the glassy phase of YSZ after aqueous exposure during our pH testing. These images show an outer zone where glass has dissolved as well as an inner zone where the interstitial glass deeper into the ceramic body has been zeolitized. Apparently, dissolution and reactions of the interstitial glass phase limit the chemical durability of such YSZ tubes, although the Nernstian behavior seems to have been intact in the present investigation until catastrophic failure of the pH sensor occurs.

### 3.3. Phase stability

The optimum phase for the YSZ tubes can be deduced from Fig. 10 (simplified by Claussen., 1984, from Stubican et al., 1984). There are three zirconia polymorphs: monoclinic (M) at low temperature, tetragonal (T) at intermediate temperatures, and cubic (C) at high temperatures, with the stability of the cubic phase increasing with higher $Y_2O_3$ content. The polymorphic transition from monoclinic to cubic increases the molar volume by 7%. Thus, for thermal shock resistance, the so-called "fully stabilized" zirconia ceramic membranes are $Y_2O_3$ solid solutions so chosen to maintain the cubic state. The optimum composition of 8 mol% $Y_2O_3$ remains cubic and avoids fracturing due to a volume change in phase transition and is also electrically responsive (Bourcier et al., 1987).

If the $Y_2O_3$ solid solution is not homogeneous within and among the grains, phase transitions and accompanying, damaging volume changes could occur due to temperature changes. In fact, secondary X-ray maps showed that the $Y_2O_3$ is not evenly distributed within the $ZrO_2$ grains of some types of
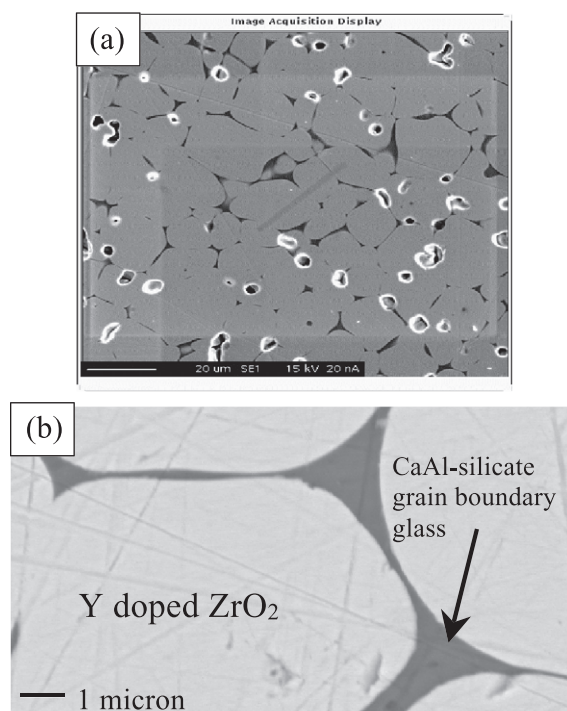


Fig. 7. (a) A wide-area secondary electron, microprobe image of a commercial YSZ tube showing the intergranular glass phase and pores (bright areas) in the $ZrO_2$ ceramic. (b) An SEM image showing the glass phase present at all $ZrO_2$ grain boundaries. Note the 20- and 1-μm scale bars.
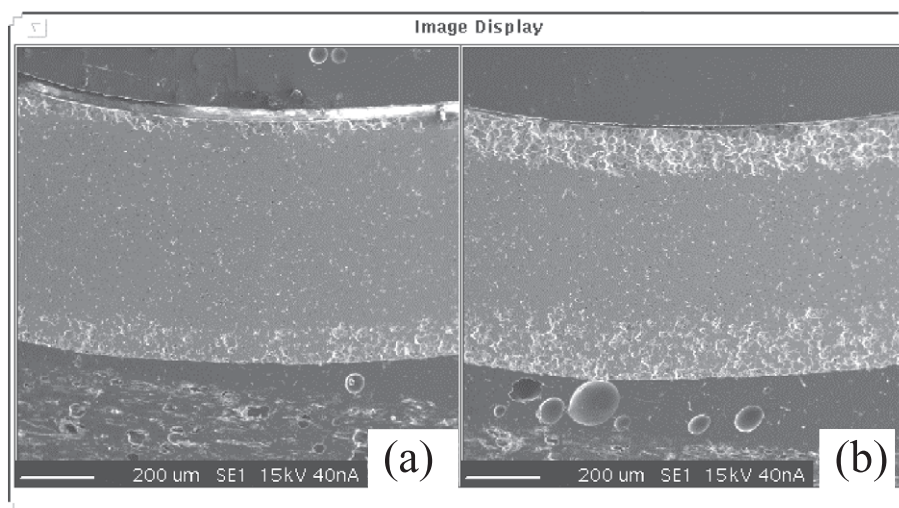
Fig. 8. Textures of cross-sections of the YSZ tubes after acid dissolution at the Ca–Al–silicate grain boundaries. Glass dissolution is shown by roughened layers on the inner and outer curved surfaces and by microcracks visible as fine wire lies: (a) damage to the outer convex membrane surface from the hydrothermal tests is shown in Figs. 3 and 4; (b) a tube soaked in hot, boiling concentrated HCl for 10 min with resulting damage to both inner and outer surfaces. Spherical forms at the bottom of the sections are bubbles in the mounting media. Note the 200-μm scale bars.

commercial YSZ. Consequently, the membrane may not have been fully stabilized against thermal shock, thereby accounting for failure of tubes in furnaces where the thermal gradients were largest even though the membranes were equilibrated below 400 °C.

The impedances of the polymorphs of these compounds (Bonanos et al., 1984) apparently increase from tetragonal to cubic to monoclinic. Thus, if the YSZ is not a single polymorphic phase, its impedance will vary not only with temperature but also with polymorph, which would produce impedance discontinuities. For this reason, as well as for thermal shock stability, it is important that the YSZ sensor be entirely a single phase, preferably a cubic solid solution.

### 3.4. Charge carriers

The conductivity behavior of $ZrO_2$ is known to vary with temperature, polymorphic type, solid solution, and specific ion concentrations (Sato, 1971; Jakeš, 1969). The conductivity of $ZrO_2$ and its binary solid solutions with rare earth or alkali oxides is generally a linear function in log $R(\Omega)$ vs. reciprocal absolute temperature, $T$. Shown in Fig. 11 are the resistively data from a commercial YSZ tube used in this study. Measurements were made with Keithley 610C Electro-

meters with $10^{14}$ $\Omega$ internal impedance over the temperature range indicated in Fig. 11 in $CO_2/H_2$ mixtures of 200:1 and 100:1 (by volume). These are measurements of total impedance through the YSZ tube and both the hydrogen–platinum and Cu electrodes plus contact resistances that complete the electrical circuit. The daily variations in impedance may be due to inconsistency in the resistance of the friction-fit dry electrode contacts. However, for the V-1 type of ceramic, the log of impedance at 200 °C (10,000/$T$ = 20) in these dry measurements is ~ 10.0 (Fig. 11), as compared with the intrinsic impedance of pH-sensing YSZ electrodes in earlier KCl aqueous immersion measurements of 7.5 ± 0.5 (Bourcier et al., 1987).

As these data show, there is a linearity over a wide temperature range. As noted, if the impedance of the electrode is a simple, linear function of $1/T$, then the active charge carrier(s) is likely to be constant over that temperature range. In geoscience investigations, there have been many discoveries of mixed charge carriers: at both high and low temperature in $f_{O_2}$ sensing. Sato (1971) reviewed the literature of this entire problem and showed that many $ZrO_2$ ceramics do indeed display mixed conductivity mechanisms and that particularly at high temperature (>800 °C) and extremely reducing conditions (<iron–wustite
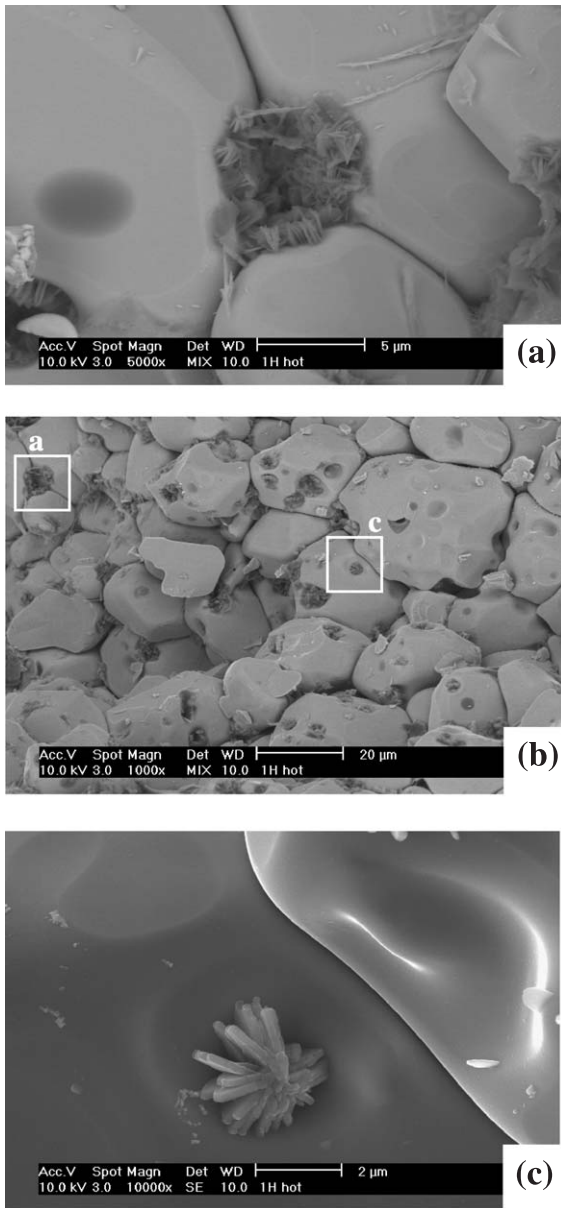
Fig. 9. SEM images of YSZ cell taken from service after several hundred hours. Images (a) and (c) are higher magnification areas of image (b). The glass phase shown in Fig. 8 and this figure has become zeolitized in the middle zone of the ceramic wall, inside the leached rim of this figure. The zeolites have not yet been identified.

equilibria), electronic conductivity (so-called, n-type semi-conduction) may be mixed with ionic conductivity. Since this Sato paper, others have specific observations, Ulmer (1984) showed that the influence

of 700 ppm $Fe^{2+}/Fe^{3+}$ contamination in $ZrO_2$ ceramics produced an n-type electronic contribution to the sensor's emf at temperatures as low as 900 °C. Burkhard and Ulmer (1995) found at temperatures lower than 300 °C a non-Nernstian behavior that they ascribed to catalytic problems at the Pt electrode and/or mixed conductivity; they did show that it was reproducible and therefore could be blank-corrected and calibrated. Mendybaev et al. (1998), while studying very reduced meteoritic phases, have discussed their successful calibration for $ZrO_2-fO_2$ sensors, despite an electronic n-type contribution.

However, there are contrasting data in the work of Park and Blumenthal (1989), who indicated that in pure $ZrO_2$, any electron mobility (n-type) or hole migration (p-type) behavior is orders of magnitude less likely than oxygen diffusion except at very high temperatures (>1000 °C) and very reducing conditions ($-\log fO_2 < 20$). Their data indicate that, even at 1000 °C, zirconia has a very wide band gap, meaning that conduction cannot be related to thermally activated electrons (n-type conductivity), nor related to migration of vacancies (p-type conductivity).

The observations of Park and Blumenthal vs. Sato and others cannot readily be reconciled as these
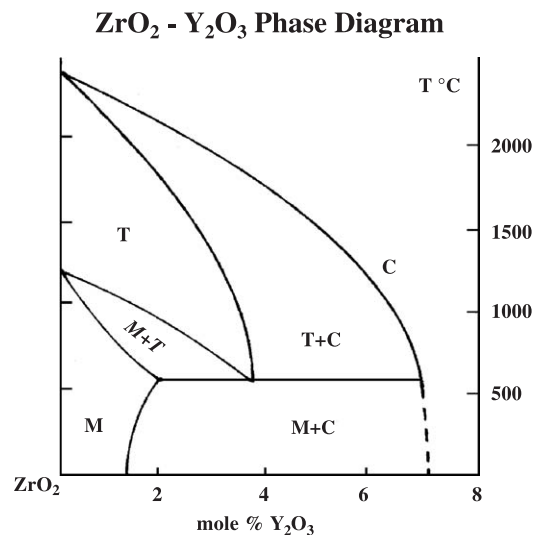


Fig. 10. A schematic phase diagram of the $ZrO_2-Y_2O_3$ binary where C = cubic, T = tetragonal, and M = monoclinic (after Claussen, 1984). For a detailed version of this phase diagram, see Stubican et al. (1984).
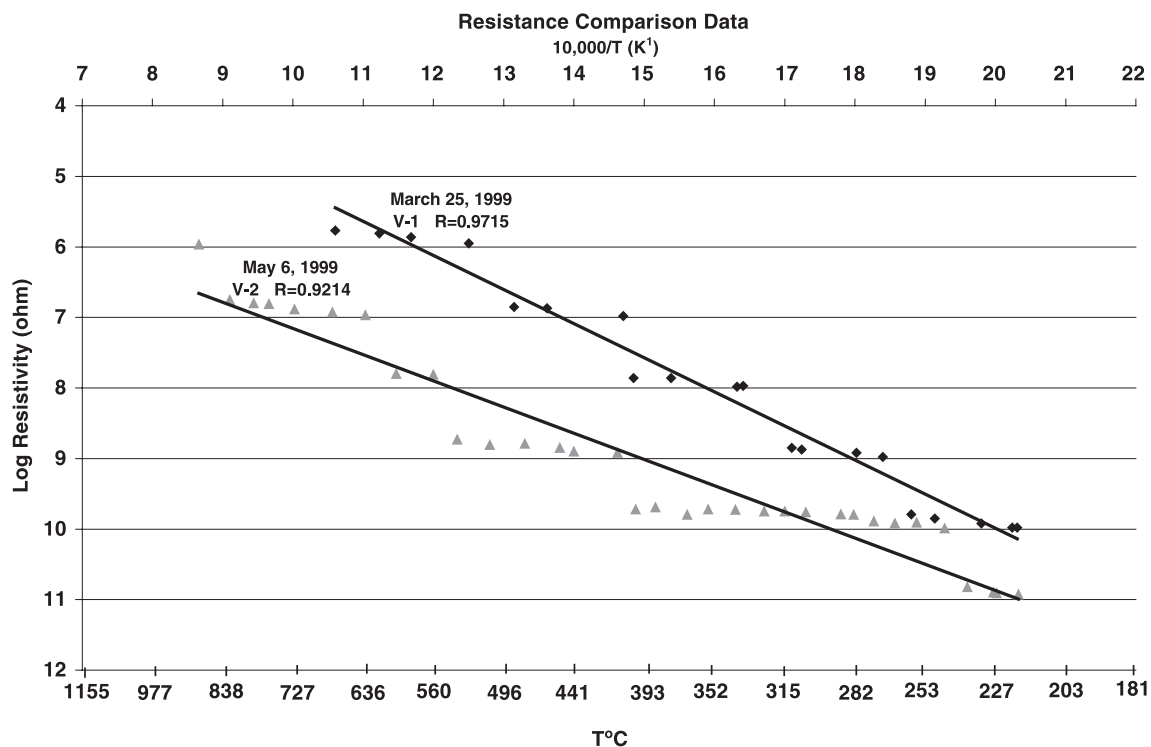
**Resistance Comparison Data**



Fig. 11. Bulk resistance of the V-1 and V-2 type of ceramics. The graph data were least-square-fit to evaluate the slopes and the possibility of a linear relationship for resistance vs. temperature. It should be noted that the data are not corrected for either circuit contact surface area or electrode geometry or contact resistance of the electrodes. Furthermore, the 'staircase pattern' suggests a nonlinearity in the meter between its decade scales over the range investigated and this is true. Keithley Electrometers 610C was employed for these measurements and Keithley confirms that their decade switch is not linearly overlapped. Within these uncertainties and within the least-squares-fit, no major slope change, i.e., no major charge carrier change seems apparent.

studies produce different results in the same temperature range. We deduce that the $ZrO_2$ ceramics used by Park and Blumenthal (1989) contained additives of the same glass as reported herein (see Figs. 8–10 and the text discussion of this glass). The manufacturer who supplied Park and Blumenthal with their ceramics used that glass in the $ZrO_2$ ceramic production from at least 1982 until the present, as we have established by examining our own labs' inventories that we had purchased over that interval from the given manufacturer. By contrast, the ceramics used by Sato, Ulmer, Burkhard and Ulmer, and Mendebaev et al. have been from the two other manufacturers who did not use the glass additive. Thus, different conclusions about the constancy of charge carrier are available in the literature. Our experimental studies

and some literature on the $ZrO_2$-based pH sensor (for example, Ding and Seyfried, 1998) advise that there is no "ceramic contribution" in total measured potential and, therefore, no test on Nerstian behavior is necessary. However, to assume that this test is not necessary may be dangerous in that the literature already contains the above disagreement over the temperature and redox range for non-mixed, constant-oxygen-ionic-charge carrier.

Moreover, even just a few hundred parts per million of redox-active impurities in the $ZrO_2$ ceramics, such as Fe or Ti, may seriously alter the oxygen diffusivity itself, as has been shown by Merino et al. (1996). Hence, one must consider the possibility that there could be a disruption to oxygen-ion-based sensor response in $ZrO_2$ ceramics with Ti or

Fe present. In exposure to geothermal well fluids, which have been shown by Gislasson and Eugster (1984) and Kacandes and Grandstaff (1989) to be at or near the (FMQ) redox state, it is well known that $Ti^{4+}$ is easily at least partially reduced (Magnelli phases) in oxide solid solutions to $Ti^{3+}$, and that $Fe^{3+}$ coexists with $Fe^{2+}$. Even if the temperature in $ZrO_2$-based pH sensors is too low to have electron hopping between these sites, Merino et al. (1996) have shown that such species can alter the oxygen-ion diffusivity without inducing any electronic charge carrier. The ceramic shown in Figs. 8–10 does indeed have several hundred parts per million of both Fe and Ti (Manna, 2002).

Another factor that may influence the oxygen diffusion and the impedance of the YSZ electrode is the influence of the solid solution composition of each phase. This effect is better studied for electrodes used specifically as oxygen sensors, but is also worth investigation for pH sensors since they also rely on oxygen diffusion. As the concentration of the $Y_2O_3$ solid solution is increased in $ZrO_2$, the effective impedance decreases (Jakeš, 1969). That is due to a charge imbalance that is compensated for by the 'omission' of oxygen as 1 mol of $Y_2O_3$ in the cubic lattice replaces $2ZrO_2$. Thus, as $Y_2O_3$ dopant is added, more vacancies are created favoring diffusion, and hence, the impedance decreases without a change in charge carrier. As $Y_2O_3$ content increases, the conductivity increases to a maximum, then decreases, presumably as 'too much' $Y_2O_3$ becomes present and locally dominates the defect concentration with its own lattice (Baumard and Abelard, 1984).

### 3.5. Textural effects on impedance

There are several textural factors that influence the impedance of YSZ sensors, as follows. Electron microprobe examination of commercial YSZ tubes has revealed compositional inhomogeneities. Furthermore, the impedance spectroscopy measurements of Butler et al. (1984), Badwal and Drennan (1988) and Badwal (1992) have demonstrated that the impedance of zirconia sensors depends upon at least four textural parameters: (1) grain geometry, (2) grain boundaries, even when clean, (3) grain boundary impurities, and (4) the contact resistance in the contacting metal electrode circuit.

The number of open, non-sintered, grain boundaries per unit volume of membrane understandably affects the overall impedance. Similarly, interstitial phases along these boundaries change the impedance as already discussed above. The impedance is increased by separation of the grain boundaries by pores, with porosities of ~ 3 to ~ 5 vol.% in the commercial YSZ tubes used here. Again, the concern is that some ceramic may not have equal oxygen electrochemical potential at both sides of the membrane.

## 4. Conclusions

Accurate pH measurements in hydrothermal systems at temperatures above 300 °C are now possible with an 8 mol% $Y_2O_3$-doped zirconia electrode used in a flow-through mode in conjunction with a flow-through external reference electrode. The significant accomplishment of this work is the development of techniques to minimize the impact of metal corrosion on pH measurement of hydrothermal solution. A recently developed flow-through YSZ sensor (Zhou et al., 2001, 2003) allows the high-temperature pH measurements to be made in a manner, in principle, similar to those made under ambient conditions comparing the pH values between test and reference solutions. In a test of this electrode system, measured was $pK_{HCl}$ with results at 320 °C of $1.46 \pm 0.46$ and at 350 °C of $2.35 \pm 0.25$, in good agreement with published values.

A precision of $\pm 0.05$ pH units is now possible in high-temperature solutions up to 350 °C when measuring hydrothermal equilibrium constants for ionization, ion-pair formation, complexation, etc., over a wide temperature and pressure range. This newly possible precision could improve thermodynamic geochemical modeling in high-temperature aqueous environments.

The limits to the utility of this pH measuring system have yet to be explored to the extent necessary for routine applications. Needed are experimental tests, among other parameters, of the combined upper thermal and upper redox limits and of the rates of dissolution of $ZrO_2$ and $Y_2O_3$ from the electrode surface for various aqueous solutions that could limit electrode life (Manna, 2002; Manna et al., 2001).

Commercial ceramics have been found to be lacking for long-term uses or for insertion into hydrothermal systems. Possible differences in composition of the commercially available $ZrO_2$ ceramics suggest that a comprehensive test is necessary before assuming that any $ZrO_2$ sensor can be used.

## Acknowledgements

## References

Aja, S.U., Wood, S.A., Williams-Jones, A.E., 1995. The aqueous geochemistry of Zr and the solubility of some Zr-bearing minerals. Appl. Geochem. 10, 603–620.

Badwal, S.P.S., 1992. Zirconia-based solid electrolytes: microstructure, stability and ionic conductivity. Solid State Ionics 52, 23–32.

Badwal, S.P.S., Drennan, J., 1988. Grain boundary resistivity in zirconia based electrolytes. Inst. Phys. Conf. Ser. 89, 277–282.

Bandura, A.V., Lvov, S.N., 2000. The ionization constants of water over a wide range of temperatures and densities. In: Tremaine, P.R., Hill, P.G., Irish, D.E., Palakrishnan, P.V. (Eds.), Steam, Water, and Hydrothermal Systems: Physics and Chemistry Meeting the Needs of Industry. NRC Press, Ottawa, pp. 96–102.

Baumard, J.F., Abelard, P., 1984. Defect structure and transport properties of ZrO2-based solid electrolytes. In: Claussen, N., Rühle, M., Heuer, A. (Eds.), Science and Technology of Zirconia II. Amer. Ceramic Soc. Advances in Ceramics, vol. 12, pp. 555–572.

Bonanos, N.R.K., Slotwinski, R.K., Steele, B.C.H., Butler, E.P., 1984. Electrical conductivity/microstructural relationships in aged CaO and calcia and magnesia partially stabilized zirconia. J. Mater. Res. 19, 785–793.

Bourcier, W.L., Ulmer, G.C., Barnes, H.L., 1987. Hydrothermal pH sensors of ZrO2, Pd hydrides, and Ir oxides. In: Ulmer, G.C., Barnes, H.L. (Eds.), Hydrothermal Experimental Techniques. Wiley-Interscience, New York, pp. 157–188.

Burkhard, D.J.M., Ulmer, G.C., 1995. Kinetics and equilibria of redox systems at temperatures as low as 300 °C. Geochim. Cosmochim. Acta 59, 699–1714.

Butler, E.P., Slotwinski, R.K., Bonanos, N.R.K., Drennan, J., Steele, B.C.H., 1984. Microstructural–electrical property relationships in high conductivity zirconias. In: Claussen, N., Rühle, M., Heuer, A. (Eds.), Science and Technology of Zirconia II. Amer. Ceramic Soc. Advances in Ceramics, vol. 12, pp. 572–584.

Claussen, N., 1984. Microstructural design of zirconia-toughened ceramics (ZTC) (1984). In: Claussen, N., Rühle, M., Heuer, A. (Eds.), Science and Technology of Zirconia II. Amer. Ceramic Soc. Advances in Ceramics, vol. 12, pp. 325–351.

Danielson, M.J., Koski, O.H., Meyers, J., 1985a. Performance improvement for high temperature stabilized-zirconia pH sensors. J. Electrochem. Soc. 132 (8), 2037–2038.

Danielson, M.J., Koski, O.H., Meyers, J., 1985b. Recent developments with high temperature stabilized-zirconia pH sensors. J. Electrochem. Soc. 132 (2), 296–301.

Ding, K., Seyfried Jr., W.E., 1995. In-situ measurement of dissolved $H_2$ in aqueous fluid at elevated temperatures and pressures. Geochim. Cosmochim. Acta 59, 4769–4773.

Ding, K., Seyfried Jr., W.E., 1996a. Direct pH measurement of NaCl-bearing fluid with in situ sensor at 400 °C and 40 megapascals. Science 272, 1634–1635.

Ding, K., Seyfried Jr., W.E., 1996b. Gold as a hydrogen sensing electrode for in situ measurement of dissolved $H_2$ in supercritical aqueous solution. J. Solution Chem. 25, 421–433.

Ding, K., Seyfried Jr., W.E., 1998. Real-time monitoring of hydrothermal vent chemistry-theory, method and applications. Long Term Monitoring of the Mid-Atlantic Ridge (MOMAR), Inter-Ridge Work Shop, Poster Abstract, Lisbon University, October 28–31, Lisbon, Portugal.

Dobson, J.V., 1972. Potentials of the palladium hydride reference electrode between 25–195 °C. J. Electroanal. Chem. 35, 129–135.

Dobson, J.V., Snodin, P.R., Thirsk, H.R., 1976. EMF measurements of cells employing metal–metal oxide electrodes in aqueous chloride and sulfate electrolytes at temperatures between 25–250 °C. Electrochim. Acta 21, 527–533.

Eklund, K., Lvov, S.N., Macdonald, D.D., 1997. The measurements of Henry's constant for hydrogen in high subcritical and supercritical aqueous systems. J. Electroanal. Chem. 437, 99–110.

German, R., 1985. Liquid Phase Sintering Plenum, New York. 240 pp.

Gislasson, S.R., Eugster, H.P., 1984. Oxygen fugacities in a basalt-meteoric water–geothermal system: Kafla, N.E. Iceland. Geol. Soc. Amer. Bull. 16, 520 (abstract).

Gouma, P.I., Akbar, S.A., Mills, M.J., 1998. Microstructural characterization of sensors based on electron ceramic materials. Journal of the Minerals, Metals, and Materials Society (JOMe).

http://www.tms.org/pubs/journals/JOM/9811/Gouma/Gouma-9811.html, 15 pp.

Haselton Jr., H.T., Cygan, G.L., Jenkins, D.M., 1995. Experimental study of muscovite stability in pure water and 1 molal KCl–HCl solutions. Geochim. Cosmochim. Acta 59, 429–442.

Hettiarachchi, S., Macdonald, D.D., 1984. Ceramic membranes for precise pH measurements in high temperature aqueous environments. J. Electrochem. Soc. 131 (9), 2206–2207.

Hettiarachchi, S., Kedzierzawski, P., Macdonald, D.D., 1985. pH measurements of high temperature aqueous environments with stabilized-zirconia membranes. J. Electrochem. Soc. 132, 1866–1870.

Hettiarachchi, S., Mekela, K., Song, H., Macdonald, D.D., 1992. The viability of pH measurements in supercritical aqueous systems. J. Electrochem. Soc. 139, L3–L4.

Jakeš, D., 1969. Galvanické clanky s pevnymi electrolyte. Chem. Listy 63, 1073–1091.

Kacandes, G.H., Grandstaff, D.E., 1989. Differences between geothermal and experimentally derived fluids: how well do hydrothermal experiments model the composition of geothermal reservoir fluids. Geochim. Cosmochim. Acta 52, 343–358.

Klein, S.A., Harvey, A.H., 1996. NIST/ASME Steam Properties, NIST Standard Reference Database 10, Version 2.0, NIST, Gaithersburg.

Kriksunov, L.B., Macdonald, D.D., 1995. Advances in measuring chemistry parameters in high temperature aqueous systems. In: White, H.J., Sengers, J.V., Neummann, D.B., Bellow, J.C. (Eds.), Phys. Chem. of Aqueous Systems. Begell House, New York, pp. 432–440.

Kriksunov, L.B., Macdonald, D.D., Millitt, P.J., 1994. Tungsten/tungsten oxide pH sensing electrode for high temperature aqueous environments. J. Electrochem. Soc. 141, 3002–3005.

Lvov, S.N., Macdonald, D.D., 1996. Estimation of the thermal liquid junction potential of an external pressure balanced reference electrode. J. Electroanal. Chem. 403, 25–30.

Lvov, S.N., Macdonald, D.D., 1997. Potentiometric studies of supercritical water chemistry. In: Spear, K.E. (Ed.), High Temperature Materials Chemistry. Electrochem. Society, Pennington, NJ, pp. 747–755.

Lvov, S.N., Zhou, X.Y., 1998. pH measurements in supercritical hydrothermal systems. Mineral. Mag. 62A, 929–930.

Lvov, S.N., Perboni, G., Broglia, M., 1995. High temperature pH measurements in dilute aqueous ammonia solutions. In: White, H.J., Sengers, J.V., Neumann, D.B., Bellows, J.C. (Eds.), Physical Chemistry of Aqueous Systems. Begell House, New York, pp. 441–448.

Lvov, S.N., Gao, H., Macdonald, D.D., 1998a. Advanced flow-through external pressure-balanced reference electrode for potentiometric and pH studies in high temperature aqueous solutions. J. Electroanal. Chem. 443, 186–194.

Lvov, S.N., Gao, H., Kouznetsov, D., Balachov, I., Macdonald, D.D., 1998b. Potentiometric pH measurements in high subcritical and supercritical aqueous solutions. Fluid Phase Equilib. 150/151, 515–523.

Lvov, S.N., Zhou, X.Y., Macdonald, D.D., 1999. Flow-through electrochemical cell for accurate pH measurements at temperatures up to 400 °C. J. Electroanal. Chem. 463, 146–156.

Lvov, S.N., Zhou, X.Y., Ulyanov, S.M., Gao, H., Macdonald, D.D., 2000a. Potentiometric measurements of association constant and pH in HCl(aq) high temperature solutions. In: Tremaine, P.R., Hill, P.G., Irish, D.E., Palakrishnan, P.V. (Eds.), Steam, Water, and Hydrothermal Systems: Physics and Chemistry Meeting the Needs of Industry. NRC Press, Ottawa, pp. 653–660.

Lvov, S.N., Zhou, X.Y., Ulyanov, S.M., Bandura, A.V., 2000b. Reference system for assessing viability and accuracy of pH sensors in high temperature subcritical and supercritical aqueous solutions. Chem. Geol. 167, 105–115.

Macdonald, D.D., Owen, D., 1973. Transport number for hydrochloric acid at elevated temperature. Can. J. Chem. 51, 2747–2749.

Macdonald, D.D., Butler, P., Owen, D., 1973a. Hydrothermal hydrolysis of $Al^{3+}$ and precipitation of boehmite from aqueous solutions. J. Phys. Chem. 77, 2474–2479.

Macdonald, D.D., Butler, P., Owen, D., 1973b. High temperature aqueous electrolyte concentration cells and the ionization of liquid water to 200 °C. Can. J. Chem. 51, 2590–2595.

Macdonald, D.D., Scott, A.C., Wentrcek, P.R., 1979a. Silver/silver chloride thermocells and thermal liquid junction potentials for potassium chloride solutions at elevated temperatures. J. Electrochem. Soc. 126 (9), 1618–1624.

Macdonald, D.D., Scott, A.C., Wentrcek, P.R., 1979b. External reference electrodes for use in high temperature aqueous systems. J. Electrochem. Soc. 126, 908.

Macdonald, D.D., Wentrcek, P.R., Scott, A.C., 1980. The measurement of pH in aqueous systems at elevated temperatures using palladium hydride electrodes. J. Electrochem. Soc. 127, 1745–1751.

Macdonald, D.D., Hettiarachchi, S., Lenhart, S., 1988. The thermodynamic viability of yttria-stabilized pH sensors for high temperature aqueous solutions. J. Solution Chem. 17, 719–732.

Macdonald, D.D., Hettiarachchi, S., Song, H., Makela, K., Emerson, R., Haim, M., 1992. Measurements of pH in subcritical and supercritical aqueous systems. J. Solution Chem. 21, 849–881.

Manna, M., 2002. Zirconium Oxide–Yttrium Oxide $fO_2$/pH Electrode Behavior: The Role of Temperature on Acid Durability. Department of Geology, Temple University, 169 pp.

Manna, M.F., Grandstaff, D.E., Ulmer, G.C., Vicenzi, E.P., 2001. The chemical durability of yttria-stabilited ZrO2 pH and O2 geothermal sensors. In: Cidu, R. (Ed.), Proceedings of the Tenth International Symposium on Water–Rock Interaction. Balkema, Rotterdam, The Netherlands, pp. 295–299.

Mendybaev, R.A., Beckett, J.R., Stolper, E., Grossman, L., 1998. Measurement of oxygen fugacities under reducing conditions. Non-Nernstian behavior of $Y_2O_3$-doped zirconia sensors. Geochim. Cosmochim. Acta 62, 3131–3139.

Merino, R.I., Nicoloso, N., Maier, J., 1996. Nature of the electronic defects in yttria-stabilized zirconia and their influence on oxygen diffusion. In: Steele, B.C.H. (Ed.), Ceramic Oxygen Ion Conductors and Their Technological Applications. Institute of Materials, University Press, Cambridge, UK, pp. 43–52.

Mesmer, R.E., Holmes, H.F., 1992. pH definition and measurement at high temperatures. J. Solution Chem. 21, 725–744.

Mesmer, R.E., Baes Jr., C.F., Sweeton, F.H., 1970. Acidity measurements at elevated temperatures: IV. Apparent dissociation of

water in 1m potassium chloride up to 292 °C. J. Phys. Chem. 74, 1937–1954.

Mesmer, R.E., Palmer, D.A., Wesolowski, D.J., 1995. Potentiometric studies at ORNL with hydrogen electrode concentration cells. In: White, H.J., Sengers, J.V., Neumann, N.B., Bellows, J.C. (Eds.), Physical Chemistry of Aqueous Systems: Meeting the Needs of Industry. Begell House, New York, pp. 423–431.

Niedrach, L.W., 1980a. A new membrane-type pH sensor for use in high temperature–high pressure water. J. Electrochem. Soc. 127, 2122–2130.

Niedrach, L.W., 1980b. Oxygen ion conducting ceramics: a new application in high temperature–high pressure pH sensors. Science 207, 1200–1202.

Niedrach, L.W., 1981. Hydrogen ion electrode having a membrane of an oxygen ion conducting ceramic. U.S. Patent 4, 264, 424, Assignee: General Electric, April 28, 1981, 8 pp. and 5 drawings.

Niedrach, L.W., 1982. Use of a high temperature pH sensor as a "Pseudo-Reference-Electrode" in monitoring corrosion and redox potential at 285 °C. J. Electrochem. Soc. 212, 672–684.

Niedrach, L.W., 1984. Application of zirconia membranes as high temperature pH sensors. Adv. Ceram. Sciences 12, 672–684.

Niedrach, L.W., Stoddard, W.H., 1984. Development of a high temperature pH electrode for geothermal fluids. J. Electrochem. Soc. 131, 1017–1026.

Pang, J., Macdonald, D.D., Millett, P.J., 1993. Acid/base titrations of simulated PWR crevice environments. Proc. Sixth Int. Symp. Environ. Degrad. Maters. Nucl. Power Systs.-Water Reactors, August 1–5, San Diego, CA. National Association of Corrosion Engineers, International (NACE International), Houston, TX, pp. 923–927.

Park, J.-H., Blumenthal, R.N., 1989. Electronic transport in 8 mole percent $Y_2O_3$–$ZrO_2$. J. Electrochem. Soc. 136, 2867–2876.

Polster, W., Barnes, H.L., 1994. Comparative hydrodynamic and thermal characteristics of sedimentary basins and geothermal systems in sediment-filled rift valleys. In: Ortoleva, P. (Ed.), Basin Compartments and Seals. Am. Assoc. of Petroleum Geologists Mem., vol. 61, pp. 437–457.

Sato, M., 1971. Electrochemical measurements and control of oxygen fugacities and other gaseous fugacities with solid electrolyte sensors. In: Ulmer, G.C. (Ed.), Research Techniques for High Temperature and High Pressure. Springer-Verlag, New York, pp. 43–99.

Schoonen, M.A.A., Barnes, H.L., 1997. Chemical and physical data for hydrothermal systems. Appendix A. In: Barnes, H.L. (Ed.), Geochemistry of Hydrothermal Ore Deposits, 3rd ed. Wiley-Interscience, New York, pp. 937–962.

Seward, T.M., Barnes, H.L., 1997. Ore minerals, transport, and deposition. In: Barnes, H.L. (Ed.), Geochemistry of Hydrothermal Ore Deposits, 3rd ed. Wiley-Interscience, New York, pp. 486–535.

Shock, E.L., Sassani, D.C., Willis, M., Sverjensky, D., 1997. Inorganic species in geologic fluids: correlations among standard molal thermodynamic properties of aqueous ions and hydroxide complexes. Geochim. Cosmochim. Acta 51, 907–950.

Stubican, V.S., Corman, G.S., Hellamn, J.R., Senft, G., 1984. Phase relationships in some $ZrO_2$ systems. Science and Technology of Zirconia. Advances in Ceramics, vol. 12, pp. 96–107.

Sweeton, F.H., Mesmer, R.E., Baes Jr., C.F., 1973. A high-temperature flowing EMF cell. J. Phys. E 6, 165–168.

Tsuruta, D., Macdonald, D.D., 1981. Measurement of pH and potential in boric acid/lithium hydroxide buffer solutions at elevated temperatures. J. Electrochem. Soc. 128, 1199–1203.

Tsuruta, T., Macdonald, D.D., 1982. Stabilized ceramic membrane electrodes for the measurement of pH at elevated temperatures. J. Electrochem. Soc. 129, 1202–1210.

Ulmer, G.C., 1984. $ZrO_2$ oxygen and hydrogen sensors: a geologic perspective. Adv. Ceram. Sciences 12, 660–671.

Wesolowski, D.J., Palmer, D.A., Mesmer, R.E., 1995. Measurements and control of pH in hydrothermal solutions. In: Kharaka, Y.K., Chudaev, O.V. (Eds.), Water–Rock Interaction. Balkema, pp. 51–55.

Wood, R.H., Hnedkovsky, L., Lin, C.L., Shock, E.L., 1991. Development of an experimental data base and theories for prediction of thermodynamic properties of aqueous electrolytes and nonelectrolytes of geochemical significance at supercritical temperatures and pressures. Proc. of the Sedimentory Basin Geochemistry and Fluid/Rock Interactions Workshop, Oklahoma.

Zhou, X.Y., Bandura, A.V., Ulyanov, S.M., Lvov, S.N., 2000. Calculation of diffusion potentials in aqueous solutions containing HCl, NaOH, and NaCl at temperatures from 25 to 400 °C. In: Tremaine, P.R., Hill, P.G., Irish, D.E., Palakrishnan, P.V. (Eds.), Steam, Water, and Hydrothermal Systems: Physics and Chemistry Meeting the Needs of Industry. NRC Press, Ottawa, pp. 480–487.

Zhou, X.Y., Ulyanov, S.M., Lvov, S.N., 2001. Advanced Yittria-Stabilized Zirconia pH Sensing Electrode for Chemistry Monitoring in SCWO Environments. CORROSION/2001, Paper 359, NACE, Houston, Texas.

Zhou, X.Y., Lvov, S.N., Ulyanov, S.M., 2003. Yttria-Stabilized Zirconia Membrane Electrode, US Patent #6, S17, 694.

Zimmerman, G.H., Gruszkiewicz, M.S., Wood, R.H., 1995. New apparatus for conductance measurements at high temperatures: conductance of aqueous solutions of LiCl, NaCl, NaBr, and CsBr at 28 MPa and water densities from 700 to 260 kg m$^{-3}$. J. Phys. Chem. 99, 11612–11625.